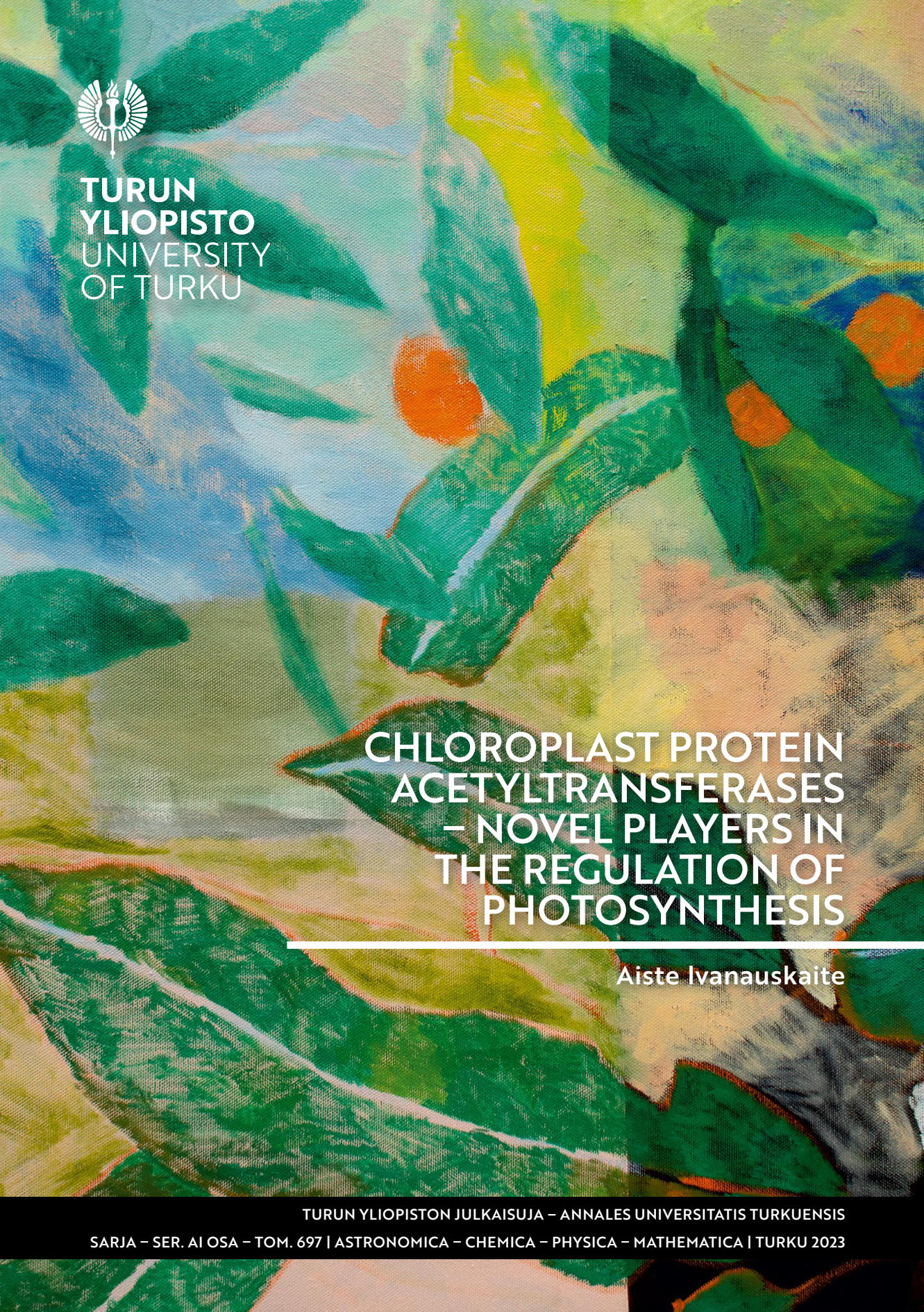

TURUN YLIOPISTO
UNIVERSITY OF TURKU

CHLOROPLAST PROTEIN ACETYLTRANSFERASES – NOVEL PLAYERS IN THE REGULATION OF PHOTOSYNTHESIS

Aiste Ivanauskaite

TURUN YLIOPISTON JULKAISUJA – ANNALES UNIVERSITATIS TURKUENSIS
SARJA – SER. AI OSA – TOM. 697 | ASTRONOMICA – CHEMICA – PHYSICA – MATHEMATICA | TURKU 2023

TURUN
YLIOPISTO
UNIVERSITY
OF TURKU

CHLOROPLAST PROTEIN ACETYLTRANSFERASES – NOVEL PLAYERS IN THE REGULATION OF PHOTOSYNTHESIS

Aiste Ivanauskaite

TURUN YLIOPISTON JULKAISUJA – ANNALES UNIVERSITATIS TURKUENSIS
SARJA – SER. AI OSA – TOM. 697 | ASTRONOMICA – CHEMICA – PHYSICA – MATHEMATICA | TURKU 2023

University of Turku

Faculty of Technology
Department of Life Technologies
Molecular Plant Biology
Doctoral programme in Technology

Supervised by

Professor Paula Mulo
Department of Life Technologies
University of Turku

Reviewed by

Docent Alexey Shapiguzov
Faculty of Biological and Environmental Sciences, University of Helsinki
Production Systems Unit, Natural Resources Institute Finland

Professor Laura Jaakola
Department of Arctic and Marine Biology
The Arctic University of Norway

Opponent

Assistant Professor Emilie Wientjes
Laboratory of Biophysics
Wageningen University

The originality of this publication has been checked in accordance with the University of Turku quality assurance system using the Turnitin OriginalityCheck service.

Cover Image: Detail of a painting, Lotta Pasila, Untitled, 2022
Oil on canvas, 110 x 145 cm

ISBN 978-951-29-9357-4 (PRINT)
ISBN 978-951-29-9358-1 (PDF)
ISSN 0082-7002 (Print)
ISSN 2343-3175 (Online)
Painosalama, Turku, Finland 2023

“If you’re asking the question, you already have an idea about the answer.”
-A quote found on the Internet at the beginning of my PhD

UNIVERSITY OF TURKU
Faculty of Technology
Department of Life Technologies
Molecular Plant Biology
AISTE IVANAUSKAITE: Chloroplast Protein Acetyltransferases – Novel Players in the Regulation of Photosynthesis
Doctoral Dissertation, 159 pp.
Doctoral Programme in Technology
June 2023

ABSTRACT

Post-translational modifications (PTMs) of proteins such as phosphorylation have been shown to play pivotal roles in the regulation of photosynthesis. However, the study of these small modifications has long been hindered by methodological limitations. In recent years, advances in mass spectrometry methods have enabled the identification of a myriad of PTMs affecting proteins in all subcellular compartments. Especially interesting is the high prevalence of protein acetylation in the chloroplast, and more specifically in photosynthetic proteins.

The acetylation machinery in the chloroplast consists of seven acetyltransferase enzymes that belong to the General control non-repressible 5-related N-acetyltransferase (GNAT) superfamily. The chloroplast-localized GNATs (GNAT1-5, GNAT7 and GNAT10) have been shown to catalyse two types of protein acetylation reactions: the addition of an acetyl group to the free N-terminus and the acetylation of an internal lysine residue of a protein. In addition, GNAT1 and GNAT2 function as metabolite acetyltransferases in the biosynthesis of melatonin. The presence of such a versatile group of plastid-localized GNAT acetyltransferases points to the importance of this PTM in the chloroplast.

In this thesis, I have focused on elucidating the physiological role(s) of a group of the newly identified chloroplast GNAT acetyltransferases with a special focus on photosynthesis. My work has shown that GNAT2 is required for the regulation of excitation energy distribution between the photosystems through state transitions. Specifically, the formation of the PSI-LHCII complex is hindered in the *gnat2* mutant, although no defects were detected in LHCII phosphorylation, which was previously considered to be the main determinant of state transitions. Additionally, GNAT2 was shown to be essential for the dynamic responses of the thylakoid membrane to changes in light conditions. GNAT1, GNAT2, GNAT4, GNAT7 and GNAT10 have a marked effect on the metabolome of *Arabidopsis thaliana*, especially on the accumulation of oxylipins, lipids and two acetylated amino acids. Finally, I have characterized two previously unknown thylakoid membrane proteins acetylated by GNAT2 and revealed their involvement in the dynamic adjustment of the light harvesting antenna of photosystem II.

KEYWORDS: Post-translational modifications, protein acetylation, GNAT acetyltransferases, photosynthesis.

TURUN YLIOPISTO
Teknillinen tiedekunta
Bioteknologian laitos
Molekulaarinen kasvibiologia
AISTE IVANAUSKAITE: Chloroplast Protein Acetyltransferases – Novel Players in the Regulation of Photosynthesis
Väitöskirja, 159 s.
Teknologian tohtoriohjelma
Kesäkuu 2023

TIIVISTELMÄ

Entsyymien aktiivisuutta sekä proteiinien lokalisaatiota ja vuorovaikutuksia säädellään erilaisten proteiinien entsymaattisten muokkausten avulla. Fotosynteesireaktioiden säätelyssä proteiinien fosforylaatio on tärkein tunnettu proteiinimuokkaus, jonka on osoitettu olevan muun muassa valohaaviproteiinien ja valoenergian keräyksen säätelyn edellytys nopeasti muuttuvissa valo-olosuhteissa. Proteiinimuokkausten tutkimus on ollut menetelmällisesti haastavaa, mutta massaspektrometriamenetelmien kehitys viime vuosina on mahdollistanut lukuisten uusien proteiinimuokkausten tunnistamisen solun eri osissa. Proteiinien asetylaatiota esiintyy erityisen runsaasti kasvin viherhiukkasissa, mutta sen mahdollinen rooli fotosynteesin säätelijänä tunnetaan huonosti.

Viherhiukkasessa asetylaatioreaktioita katalysoi seitsemän General control non-repressible 5-related N-asetyyltransferaasien (GNAT) -ryhmään kuuluvaa entsyymiä: GNAT1-5, GNAT7 sekä GNAT10. Tämän tutkimuksen tavoitteena on ollut selvittää viherhiukkasen GNAT-asetyylitransferaasien fysiologista roolia kasvissa, sekä erityisesti niiden vaikutusta fotosynteesireaktioihin. Väitöskirjatyössäni osoitan, että GNAT2-asetyyltransferaasi osallistuu fosforylaation ohella valon keräyksen säätelyyn ja viritysenergian tasapainotukseen. GNAT2 vaikuttaa myös merkittävästi tylakoidikalvoston rakenteeseen ja kalvoston rakenteen dynamiikkaan muuttuvissa valo-olosuhteissa. Osoitan myös, että proteiinien asetylaation lisäksi GNAT1-, GNAT2-, GNAT4-, GNAT7- ja GNAT10-entsyymit vaikuttavat huomattavasti lituruohon metabolomiin. Erityisesti oxylipiinien, antioksidanttina toimivan askorbaatin ja eräiden kalvolipidien määrät ovat muuttuneet tutkituissa *gnat*-mutanttilinjoissa. Lisäksi osoitan, että kaksi aiemmin tuntematonta kloroplastiproteiinia, ALM-A ja ALM-B, jotka ovat GNAT2-entsyymin mahdollisia kohdeproteiineja, osallistuvat fotosysteemi II:n valohaavin koon säätelyyn.

ASIASANAT: Proteiinimuokkaus, proteiinien asetylaatio, GNAT asetyylitransferaasit, fotosynteesi.

Table of Contents

Abbreviations

13-LOX	13-lipoxygenase
5-MT	5-methoxytryptamine
acetyl-CoA	Acetyl coenzyme A
ALM-A/B	Acetylated Little Membrane protein A/B
Arabidopsis	*Arabidopsis thaliana*
ATP	Adenosine triphosphate
ATPase	ATP synthase
BLASTp	Basic local alignment search tool for proteins
C	PSII core monomer
CBB	Calvin-Benson-Bassham cycle
CD	Circular dichroism
CET	Cyclic electron transfer
Cyt b_6f	Cytochrome b_6f
DG	Diacylglycerol
DGDG	Digalactosyldiacylglycerol
dnOPDA	Dinor-12-oxophytodienoic acid
E.coli	*Escherichia coli*
EpKODE	Epoxy-keto-octadecadienoic acid
ETC	Electron transfer chain
Fd	Ferredoxin
FNR	Fd-NADPH-oxidoreductase
FTSH	FtsH protease
Fv/Fm	Maximal PS II quantum yield
GCN5	General control non-repressible 5
gH^+	Proton conductivity
GL	Growth light
GNAT	General control non-repressible 5-related N-acetyltransferase
HL	High light
HpOTrE	Hydroperoxyoctadecatrienoic acid
JA	Jasmonic acid
K	Lysine

KAT	Lys-acetyltransferase
LCNP	Plastid lipocalin
Lhcb	Light harvesting complex II subunit
LHCI	Light harvesting complex I
LHCII	Light harvesting complex II
L-LHCII	Loosely bound LHCII
LPG 18:3	Lysophosphatidylglycerol
Lys	Lysine
MGDG	Monogalactosyldiacylglycerol
M-LHCII, M	Moderately bound LHCII
$NADP^+$	Nicotinamide adenine dinucleotide phosphate, oxidized
NADPH	Nicotinamide adenine dinucleotide phosphate, reduced
NAT	N-terminal acetyltransferase
NDH	Chloroplast NADH dehydrogenase-like complex
NPQ	Non-photochemical quenching
NSI	Nuclear Shuttle Interacting
NTRC	NADPH-dependent chloroplast thioredoxin reductase
OEC	Oxygen evolving complex
OxoOTrE	Oxo-octadecatrienoic acid
P-	Phosphate group
p300/CBP	CREB-binding protein
$P680/P680^+$	Red/ox primary electron donor of PSII
$P700/P700^+$	Red/ox primary electron donor of PSI
PBCP	PSII core phosphatase
PCR	Polymerase chain reaction
PGR5	Proton Gradient Regulation 5
PGRL1	PGR5-like 1
pmf	Proton motive force
PPFD	Photosynthetic photon flux density
PQ_A	Plastoquinone A
PQ_B	Plastoquinone B
PQ_BH_2	Plastoquinol B
PSI	Photosystem I
PSII	Photosystem II
PTM	Post-translational modification
PTOX	Plastid terminal oxidase
PUFA	Polyunsaturated fatty acid
PVDF	Polyvinylidene fluoride
QTOF–MS	Quadrupole time-of-flight mass spectrometry
RCA	Rubisco activase

ROS	Reactive oxygen species
RT-PCR	Reverse transcriptase PCR
Rubisco	Ribulose 1,5-bisphosphate carboxylase/oxygenase
S-LHCII, S	Strongly bound LHCII
SNAT	Serotonin N-acetyltransferase
STN7	State Transition 7 kinase
STN8	State Transition 8 kinase
T	Threonine
TRX	Thioredoxin
UHPLC	Ultra-high-performance liquid chromatography
UPLC-MS	Ultra-performance liquid chromatography mass spectrometry
VDE	Violaxanthin de-epoxidase
vH^+	Proton flux
Y(II)	Effective PS II quantum yield
Y(NO)	Quantum yield of nonregulated energy dissipation
YFP	Yellow Fluorescent Protein

List of Original Publications

This dissertation is based on the following original publications, which are referred to in the text by their Roman numerals:

I Koskela M.M., Brünje A., Ivanauskaite A., Grabsztunowicz M., Lassowskat I., Neumann U., Dinh T.V., Sindlinger J., Schwarzer D., Wirtz M., Tyystjärvi E., Finkemeier I. and Mulo P. Chloroplast acetyltransferase NSI is required for state transitions in *Arabidopsis thaliana*. *Plant Cell,* 2018; 30: 1695-1709.

II Rantala M., Ivanauskaite A., Laihonen L., Kanna S.D., Ughy B. and Mulo P. Chloroplast acetyltransferase GNAT2 is involved in the organization and dynamics of thylakoid structure. *Plant and Cell Physiology,* 2022; 63: 1205-1214.

III Ivanauskaite A., Rantala M., Laihonen L., Konert M.M., Schwenner N., Mühlenbeck J., Finkemeier I. and Mulo P. Loss of chloroplast GNAT acetyltransferases results in distinct metabolic phenotypes in Arabidopsis. *Plant and Cell Physiology*, 2023; 64: 549-563.

IV Ivanauskaite A., Rantala M., Konert M.M., Laihonen L., Turunen O., Vakal S., Salminen T.A., Tyystjärvi T. and Mulo P. Acetylated Little Membrane proteins A (ALM-A) and B (ALM-B) bind to M-LHCII and are required for the adjustment of the PSII antenna size in *Arabidopsis thaliana. Manuscript.*

1 Introduction

1.1 Photosynthesis

Almost all life on Earth depends either directly or indirectly on photosynthesis, which produces the reduced carbon needed to fuel the cellular reactions and provide building material for the organism. During oxygenic photosynthesis, light energy from the sun together with water are used to reduce inorganic carbon dioxide to organic carbohydrates, while oxygen is formed as a side product. Thus, in addition to energy and building blocks, photosynthesis provides the molecular oxygen that is essential for most heterotrophic organisms.

Oxygenic photosynthesis first evolved in cyanobacteria around 3.5 billion years ago, marking the start of the oxygenic burst and the formation of the atmosphere as we know it (Fischer et al., 2016). Later on, as a result of endosymbiosis, an early cyanobacteria was engulfed by a heterotrophic cell paving the way to the evolution of other photosynthetic organisms, algae and plants (Archibald, 2015). The engulfed cyanobacteria evolved into a semi-autonomous organelle, the chloroplast. While the main components of the photosynthetic machinery have remained largely unchanged since photosynthesis first evolved, evolutionary distinct photosynthetic organisms differ in the regulatory mechanisms that have enabled their adaptation to ever-changing environments. Decades of research have help us further our understanding of photosynthesis greatly, but especially the regulatory aspects of photosynthesis hold many unanswered questions to this day.

As humans we rely on photosynthesis to produce food and feed (and oxygen) that both are becoming more scarce as the human population increases. Additionally, climate change is providing new challenges for our crops as extreme weather conditions such as heat, flooding and drought are becoming more frequent. Understanding photosynthesis and especially it's regulation can help us find ways to deal with challenges of food security as well as fuel production.

In plants, photosynthesis takes place in the chloroplast, a semi-autonomous organelle surrounded by two layers of membranes: the outer and inner envelope membrane. In addition, the chloroplast holds within membrane-surrounded sacs called the thylakoids. Thylakoids are arranged as stacks of appressed membranes referred to as the grana thylakoids and the non-stacked stroma lamellae structures

that connect the grana stacks to each other. The area at the interconnection of the grana stacks and stroma thylakoids is referred to as the grana margins that together with stroma lamellae and grana tops comprises the non-appressed regions of the thylakoid membrane. The soluble compartment enclosed by the thylakoid membranes is the lumen. The overall three-dimensional ultrastructure of the thylakoid membrane is somewhat unclear, but according to the most widely accepted model, the stroma lamellae wrap helically around the stacked grana (Mustárdy & Garab, 2003; Paolillo, 1970; Ruban & Johnson, 2015). The stromal helices are connected to the grana via narrow membrane slits. Thylakoid membranes harbour the protein-pigment complexes that catalyse the first steps of photosynthesis, the light reactions. The soluble space of the chloroplast surrounding the thylakoids is called the stroma and it contains the soluble protein complexes that catalyse the carbon assimilation reactions of photosynthesis.

Notably, the thylakoid protein complexes are unevenly distributed in different parts of the thylakoid membrane. Photosystem II (PSII) is mostly restricted to the stacked grana thylakoids, while photosystem I (PSI) and ATP synthase (ATPase) are found in the non-appressed stroma thylakoids (Andersson & Anderson, 1980). The cytochrome b_6f complex (Cyt b_6f), on the other hand, is most likely evenly distributed throughout the thylakoids (Anderson, 1982; Kirchhoff et al., 2017). This arrangement of the thylakoid protein complexes is referred to as lateral heterogeneity and together with the dynamics of the thylakoid membrane system, it provides a way to modulate electron transfer in response to the prevailing light conditions (Johnson & Wientjes, 2020).

1.2 Light reactions

1.2.1 The structure of photosynthetic pigment-protein complexes

The light reactions take place in the membrane-embedded protein-pigment complexes that harvest light energy and convert it to a chemical form as ATP and NADPH (**Figure 1**). In plants, light energy is harvested by the two light harvesting complexes (LHCI and LHCII), protein-pigment antenna complexes that contain chlorophyll *a* and *b*, as well as accessory carotenoid pigments. The LHCI and LHCII complexes serve as antennae for PSI and PSII, respectively, and are composed of Lhc proteins. In *Arabidopsis thaliana* (Arabidopsis), four LHCI proteins, Lhca1-4, comprise the LHCI, while LHCII is composed of the trimer-forming Lhcb1-3 proteins that are connected to the PSII core via minor, monomeric antenna proteins Lhcb4-6 (CP29, CP26 and CP24) (Crepin & Caffarri, 2018; Jansson, 1999). In

addition to PSII, the LHCII heterotrimers can also direct excitation energy to PSI (Kyle et al., 1983; Wientjes et al., 2013).

The reaction centre of PSII is composed of the proteins D1 (PsbA), D2 (PsbD), PsbI and the α- and β- subuntis of the Cyt b559 complex. The reaction centre is surrounded by the integral light-harvesting antenna proteins CP47 (PsbB) and CP43 (PsbC) and several small subunits that together with the reaction centre form the PSII core monomer (C) (Su et al., 2017; Van Bezouwen et al., 2017). The PSII monomer binds a high number of chlorophyll and carotenoid pigments and other cofactors. The extrinsic oxygen evolving complex (OEC) is located on the lumenal side of PSII. The functional unit of PSII is a dimer (C2) surrounded by LHCII antennae proteins that bind to the core with varying strength. The C2 core can bind up to two strongly and moderately bound LHCII trimers (S-LHCII and M-LHCII) forming a large C2S2M2 supercomplex (Caffarri et al., 2009). The S-LHCII trimers are associated to the PSII core via the monomeric Lhcb5, while the M-LHCII trimers via the monomeric Lhcb4 and Lhcb6 proteins. Additionally, the C2S2M2 can bind several loosely bound LHCII trimers (L-LHCII) that are lost during complex isolation (Ruban & Johnson, 2015).

The PSI reaction centre consists of a PsaA/PsaB heterodimer, and is surrounded by subunits PsaC-PsaL, PsaN and PsaO (Amunts et al., 2007). The PSI complex also binds several pigments molecules, including chlorophylls and carotenoids. The LHCI antenna comprising of two Lhca heterodimers, Lhca1/Lhca4 and Lhca2/Lhca3, is arranged in a half-moon shape around the PSI complex, while the subunits PsaH, PsaI, PsaL and PsaO form the docking site for L-LHCII (Jensen et al., 2004; Lunde et al., 2000).

The final pigment-protein complex involved in the photosynthetic light reactions is the $Cytb_6f$ complex that functions between the two photosystems (see section 1.2.2). The $Cytb_6f$ complex consists of Cyt f, Rieske, $Cytb_6$ and subunit IV that mediate the electron transfer reactions, as well as a number of other subunits and cofactors, including one chlorophyll and one β-carotene (Kurisu et al., 2003).

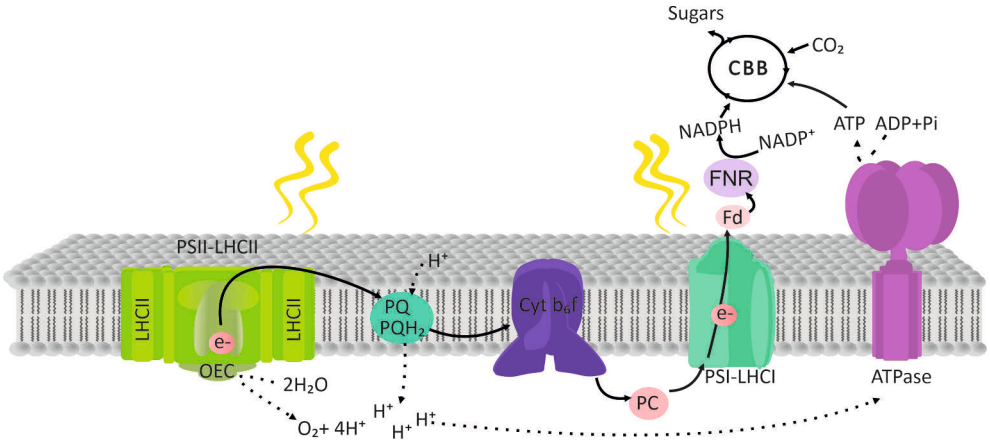

Figure 1. Schematic representation of the linear electron transfer chain catalysed by the thylakoid-embedded protein-pigment complexes (details in text). The electron and proton transfer pathways are depicted as solid and dashed arrows, respectively. Abbreviations: LHCII, light harvesting complex II; PSII, photosystem II; OEC, oxygen-evolving complex; PQ, plastoquinone; PQH_2, plastoquinol; $Cytb_6f$, cytochrome b_6f; PC, plastocyanin; PSI, photosystem I; LHCI, light harvesting complex I; Fd, ferredoxin; FNR, ferredoxin:$NADP^+$ oxidoreductase; ATPase, ATP synthase; CBB, Calvin-Benson-Bassham cycle. Figure modified from the original made by Marjaana Rantala.

1.2.2 The electron transfer chain is at the heart of the light reactions

Absorption of a photon excites an electron of a pigment to a higher energetic state and this excitation energy is transferred from one pigment molecule to another, until it reaches the reaction centre of PSII, P680. The P680 reaction centre consists of two chlorophyll *a* molecules, that when excited, readily pass an electron on to the primary electron acceptor, pheophytin, in the event of charge separation. The reduced pheophytin then transfers an electron to plastoquinone A (PQ_A), which passes the electron on to plastoquinone B (PQ_B). Once PQ_B is fully reduced by a second electron donated by a newly reduced PQ_A, PQ_B takes up two protons from the stroma forming plastoquinol (PQ_BH_2). PQ_BH_2 then detaches from PSII and diffuses in the thylakoid membrane to the plastoquinol-binding site of the Cyt b_6f complex.

$Cytb_6f$ transfers electrons from PQ_BH_2 to plastocyanin, while concomitantly translocating protons from the stroma to the lumen utilizing the Q-cycle (Malone et al., 2021). First, one electron from PQ_BH_2 is transferred via the Rieske Fe-S centre and cytochrome f to plastocyanin, a mobile electron carrier that transfers electrons from Cyt b_6f to PSI. The second electron of PQ_BH_2 is passed via two b-type heme molecules to an oxidized quinone molecule bound at the stromal side of Cyt b_6f, while the two protons of PQ_BH_2 are released into the lumen. Thus, the first round of the Q-cycle results in the oxidation of PQ_BH_2, the release of two protons into the

lumen and production of a semiquinone. When the cycle is repeated, the semiquinone is fully reduced to a plastoquinol that accepts two protons from the stroma and enters into the PQ_BH_2 pool (Malone et al., 2021).

Similarly to PSII, PSI also uses light energy to catalyse a charge separation in its reaction centre designated P700. The excited P700 readily gives an electron to the primary electron acceptor A_0 (a special form of chlorophyll), which then reduces phylloquinone A_1. The oxidized $P700^+$ is rapidly reduced by electrons from plastocyanin, while the electron from A_1 is passed through three Fe-S centers in PSI to the soluble ferredoxin (Fd) associated to the thylakoid membrane on the stromal side. Fd is oxidized by ferredoxin:$NADP^+$ oxidoreductase (FNR) and the electron is passed on to $NADP^+$, resulting in the production of NADPH. Electrons from reduced Fd can alternatively be used to reduce PQ that can be oxidized by Cyt b_6f in a process called cyclic electron transfer (CET) (**Figure 2**) (Munekage et al., 2004). CET results in the production of ATP (at the expense of NADPH) and is used to adjust the ATP/NADPH ratio according to the demands of the cell. Fd-dependent reduction of PQ can occur via two pathways: the major PGRL1/PGR5-dependent pathway or catalysed by the NADH dehydrogenase-like complex (Munekage et al., 2002, 2004; Shikanai et al., 1998). Fd also serves as an electron donor in several other reactions, such as the regulatory thioredoxin proteins and nitrogen assimilation (Hanke & Mulo, 2013).

Linear electron transfer results in the formation of the reduced electron carrier NADPH and the formation of a proton gradient across the thylakoid membrane. The latter is utilized by ATPase to produce ATP. The chloroplast ATPase consist of two domains, the transmembrane CF_0 and the peripheral CF_1 on the stromal side of the thylakoid membrane (Hahn et al., 2018). CF_1 is responsible for the formation of ATP from ADP and P_i, while CF_0 forms the proton pore across the thylakoid membrane. ATP is formed on the surface of CF_1, but its release into the stroma requires a conformational change caused by the rotation of the enzyme (Hahn et al., 2018). The energy for this rotation is obtained when protons pass through CF_0 down their electrochemical gradient.

The primary charge separation in PSII produces a very strong oxidizing agent, $P680^+$, that needs to be reduced before the complex is ready to receive a new photon. The electron for $P680^+$ reduction is obtained by the splitting of water by OEC associated to the lumenal side of PSII. The OEC catalyses the oxidation of two water molecules, which releases four electrons and protons as well as one molecule of O_2. Since water splitting releases four electrons and $P680^+$ reduction requires only one, the OEC transfers the electrons obtained from water splitting one at a time utilizing a cluster of four manganese ions, while a tyrosine residue (Tyr_Z) functions as a direct electron donor to $P680^+$. The storing and gradual passing of electrons is possible, because the manganese cluster can exist in five oxidation states (Cady et al., 2008).

Full oxidation of the manganese cluster is obtained when four photons are absorbed and four charge separations take place at P680. Once fully oxidized, the Mn-cluster is able to oxidize two water molecules to gain four electrons. Simultaneously, four protons are released into the thylakoid lumen, greatly contributing to the formation of the proton gradient across the thylakoid membrane.

1.3 Carbon assimilation reactions

The NADPH and ATP produced in the light reactions are utilized in the second part of photosynthesis, the carbon assimilation reactions. Carbon assimilation is catalysed by enzymes residing in the soluble stroma of the chloroplast and can be divided into three stages: carbon fixation, reduction and regeneration. Together, these reactions are also referred to as the Calvin-Benson-Bassham cycle (CBB) (Bassham, 1971).

The carbon fixation stage consists of one reaction, the condensation of a CO_2 molecule with a five-carbon acceptor (ribulose 1,5-bisphosphate) catalysed by ribulose 1,5-bisphosphate carboxylase/oxygenase (Rubisco) (Andersson & Backlund, 2008). The six-carbon molecule formed by Rubisco is unstable and is immediately cleaved to form two three-carbon 3-phosphoglycerate molecules (Bassham, 1971). In the following stage, reduction, 3-phosphoglycerate is first phosphorylated to produce 1,3-bisphosphoglycerate in a reaction that utilizes one molecule of ATP and is catalysed by 3-phosphoglycerate kinase. 1,3-bisphosphoglycerate is then reduced to glyceraldehyde 3-phosphate by glyceraldehyde 3-phosphate dehydrogenase and electrons from NADPH. Glyceraldehyde 3-phosphate is interconverted to dihydroxyacetone phosphate by triose phosphate isomerase.

The fixation of three CO_2 molecules and the following reduction reactions yield six three-carbon triose phosphate molecules, one of which represents the net product of carbon fixation, while the remaining five are used in the third stage of carbon assimilation reactions to regenerate three five-carbon acceptor molecules (ribulose 1,5-bisphosphate) that are ready to repeat the cycle of carbon assimilation (Bassham, 1971). The regeneration stage consists of nine steps that utilize three-, four-, five-, six-, and seven-carbon sugar intermediates and ATP. The enzymes that catalyse the regeneration reactions are: aldolase, fructose 1,6-bisphosphatase, transketolase, sedoheptulose 1,7-bisphosphatase, ribose 5-phosphate isomerase, ribulose 5-phosphate epimerase and ribulose 5-phosphate kinase (Buchanan et al., 2015). The triose phosphate molecules not used for the regeneration of ribulose 1,5-bisphosphate are used for the biosynthesis of starch for storage, converted to sucrose for transport or degraded via glycolysis for energy.

Despite of its crucial role in photosynthesis, Rubisco is a surprisingly poor catalyst of carbon fixation. The relatively low turnover rate of Rubisco is compensated by its high abundance in the chloroplast, while a second challenge caused by its faulty substrate specificity requires a more elaborate and energetically costly solution. In addition to catalysing the carboxylation of ribulose 1,5-bisphosphate using CO_2 as a substrate, Rubisco also uses O_2 as a substrate in the oxygenation of the primary carbon acceptor (Andersson & Backlund, 2008). The latter reaction results in the production of 3-phosphoglycerate and a metabolically useless molecule, 2-phosphoglycolate. 2-phosphoglycolate is converted to serine, and eventually to 3-phosphoglycerate in the glycolate pathway that requires enzymes from three different organelles: the chloroplast, peroxisome and mitochondria. One cycle of the glycolate pathway consumes one molecule of ATP and releases CO_2, thus diminishing the yield of photosynthesis. The frequency of the Rubisco-catalysed oxygenation reaction increases in higher temperatures that both decrease the solubility of CO_2 in aqueous solution and diminish the affinity of Rubisco to CO_2.

1.3.1 Regulation of carbon assimilation

Carbon assimilation is largely regulated at its first step, the fixation of CO_2 catalysed by Rubisco. In plants, Rubisco is a multimeric complex composed of eight large subunits that each contain a catalytic site and eight small subunits (Andersson & Backlund, 2008). Rubisco activity depends on the presence of a carbamoylated lysine residue and an Mg^{2+} ion in its active site. In the dark, Rubisco is readily inhibited by the binding of its substrate, ribulose 1,5-bisphophate, that in turn inhibits the nonenzymatic carbamoylation of lysine and Mg^{2+} binding. To activate Rubisco, ribulose 1,5-bisphophate is removed from the active site in an ATP-dependent reaction catalysed by Rubisco activase (RCA). RCA, on the other hand, is inhibited by the ADP formed upon Rubisco activation and is additionally regulated by its redox state via the thioredoxin system (described below), ΔpH and ATP-dependent thylakoid recruitment (Chen et al., 2010; Portis, 2003).

Because carbon assimilation requires significant amounts of NADPH and ATP that are produced in the light, several light-dependent regulatory mechanisms have evolved to activate carbon assimilation upon exposure to light. In addition to producing NADPH and ATP, the light reactions result in the increase of stromal pH from 7 to 8 and increased stromal Mg^{2+} concentration caused by the flow of Mg^{2+} ions from the thylakoids. The increase in stromal pH and Mg^{2+}, respectively, facilitate the carbamoylation of lysine and Mg^{2+} binding in the active site of Rubisco. Additionally, the activity of fructose 1,6-bisphosphatase functioning in the regeneration of ribulose 1,5-bisphosphate is highly dependent on stromal pH and Mg^{2+} concentration (Buchanan, 1980).

Another way to synchronize the activation of carbon assimilation to the light reactions is the thioredoxin-system (Nikkanen & Rintamäki, 2019). Thioredoxins (TRXs) are small soluble proteins that accept electrons from ferredoxin to reduce a disulfide bond between two of their cysteine residues. In this Fd-TRX system the reduction of thioredoxin is catalysed by ferredoxin-thioredoxin reductase. Reduced thioredoxin is then able to reduce disulfide bonds that inhibit the activity of four carbon assimilation enzymes: glyceraldehyde 3-phosphate dehydrogenase, fructose 1,6-bisphosphatase, sedoheptulose 1,7-bisphosphatase and ribulose 5-phosphate kinase (Buchanan, 2016). In the dark, the cysteine residues are again oxidized and the inhibiting disulfide bonds are formed.

While the Fd-TRX system functions predominantly in growth and high light intensities, another thioredoxin system, the NADPH-dependent chloroplast thioredoxin reductase (NTRC), is also active in the dark and lower light intensities (Nikkanen et al., 2018). NTRC receives electrons from NADPH and it combines an N-terminal thioredoxin reductase domain and a C-terminal TRX domain in a single protein. The Fd-TRX system is thought to be the primary regulator of carbon assimilation, although the NTRC systems has also been shown to affect the activity of the CBB enzymes, suggesting that the two thioredoxin systems have partially overlapping roles (Geigenberger et al., 2017; Thormählen et al., 2015).

1.4 Regulation of the light reactions

The dependence of the light reactions on the availability and quality of light means that the system needs to constantly adjust itself to adapt to the prevailing light conditions. This is no easy task, as the plants are exposed to ever-changing light conditions that can vary rapidly e.g. as a result of moving clouds or shading, or relatively slowly depending on the time of the day. Fluent and safe operation of the light reactions requires that similar amounts of light energy are directed to both photosystems, while simultaneously avoiding damage caused by excess light. To achieve this, plants have evolved several regulatory mechanisms that help to ensure efficient light harvesting, safely dissipate excess energy, protect the photosystems and redirect electrons based on the metabolic cues (**Figure 2**).

1.4.1 State transitions balance the excitation energy distribution between PSII and PSI

Due to differences in their light harvesting complexes as well as their lateral distribution in the thylakoid membrane, the two photosystems do not always receive equal amounts of excitation energy. In certain light conditions (e.g. blue or low-moderate intensity light), LHCII functions more efficiently than LHCI, thus

directing more excitation energy to PSII (Ruban & Johnson, 2009; Wientjes et al., 2013). Under such conditions the electron transfer chain (ETC) becomes reduced, and the binding of PQ_BH_2 to the $Cytb_6f$ complex leads to the activation of the serine/threonine kinase STN7, which phosphorylates LHCII proteins Lhcb1 and Lhcb2 (Bellaflore et al., 2005; Vener et al., 1997). As a result of Lhcb2 phosphorylation in the pool of L-LHCII, a specific PSI-LHCI-LHCII supercomplex is formed and more excitation energy is directed to PSI (Crepin & Caffarri, 2015; Grieco et al., 2015; Kouřil et al., 2005; Kyle et al., 1983; Pesaresi et al., 2009; Wientjes et al., 2013). In addition to Lhcb2 phosphorylation in the L-LHCII pool, also Lhcb1 found in the LHCII trimers of the PSII-LHCII supercomplexes is phosphorylated (Crepin & Caffarri, 2015; Rantala et al., 2017). LHCII phosphorylation increases the electrostatic repulsion between the PSII-LHCII supercomplexes both transversally on the opposing sides of the stromal gap as well as laterally within the thylakoid membrane (Barber, 1982; Puthiyaveetil et al., 2017). The net result of these changes is the loosening of the grana stacks, which likely allows more interaction between the protein complexes that are usually strictly restricted to different domains of the thylakoid membrane, thus facilitating the formation of the PSI-LHCI-LHCII complex (Kyle et al., 1983; Pietrzykowska et al., 2014; Rozak et al., 2002; Wood et al., 2018).

In light conditions that promote the oxidation of PQ (e.g far-red light), STN7 is inactivated and the LHCII proteins are dephosphorylated by the TAP38/PPH1 phosphatase (Pribil et al., 2010; Shapiguzov et al., 2010). Dephosphorylation of LHCII is accompanied by more compact packing of the grana stacks and a decrease in excitation energy transfer from L-LHCII to PSI (Bellaflore et al., 2005; Kyle et al., 1983; Wood et al., 2018). However, the redox state of the ETC is not the only determinant of STN7 activity, which is also inhibited by the accumulation of reduced thioredoxins in high light intensities that fully reduce the ETC (Ancín et al., 2019; Nikkanen et al., 2018; Rintamäki et al., 2000).

Reversible phosphorylation of the LHCII proteins and state transitions are especially important in the acclimation to fluctuating light conditions where lower intensity light periods are interrupted by shorter bursts of high light. This is evidenced by the retarded growth phenotype of the *stn7* mutant observed when grown under fluctuating light but absent under constant light conditions (Tikkanen et al., 2010).

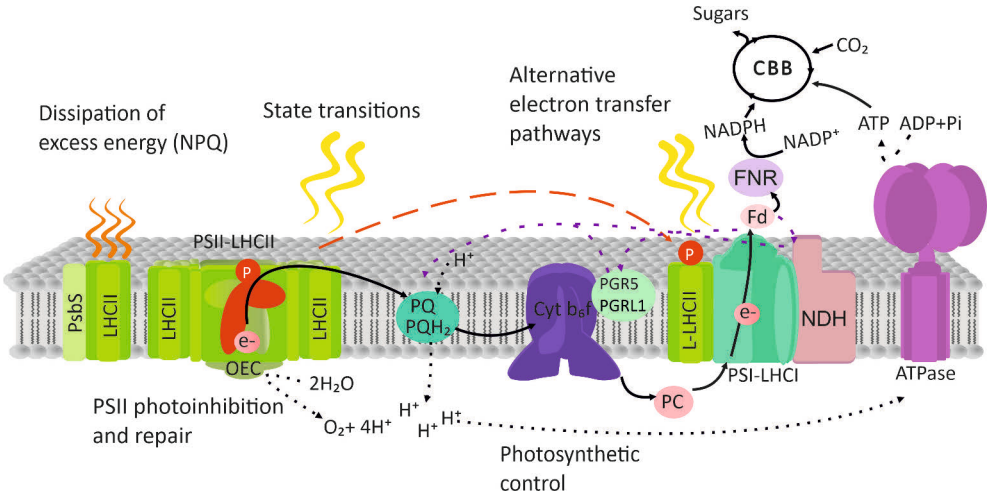

Figure 2. Simplified scheme of the regulatory mechanisms of the light reactions. The electron and proton transfer pathways are depicted as solid and black dashed arrows, respectively. Alternative electron transfer pathways are depicted as purple dashed arrows (details in text). Abbreviations: NPQ, non-photochemical quenching; LHCII, light harvesting complex II; PSII, photosystem II; OEC, oxygen-evolving complex; PQ, plastoquinone; PQH_2, plastoquinol; $Cytb_6f$, cytochrome b_6f; PGR5, Proton Gradient Regulation 5; PGRL1, PGR5-like 1; PC, plastocyanin; L-LHCII, loosely bound LHCII; PSI, photosystem I; LHCI, light harvesting complex I; Fd, ferredoxin; FNR, ferredoxin:$NADP^+$ oxidoreductase; NDH, chloroplast NADH dehydrogenase-like complex; ATPase, ATP synthase; CBB, Calvin-Benson-Bassham cycle. Figure modified from the original made by Marjaana Rantala.

1.4.2 Non-photochemical quenching of excess light energy

Excess light can lead to the production of reactive oxygen species (ROS) and result in cell damage. Thus, several protective mechanisms have evolved to dissipate excess excitation energy safely, mostly as heat. Together, these mechanisms are called non-photochemical quenching (NPQ), as opposed to photochemical quenching of chlorophyll fluorescence by PSII, and as their name implies, they can be observed by a decrease in chlorophyll fluorescence. The different components of NPQ can be separated by the timescale it takes for them to activate and relax, as well as the molecular players involved. Despite the existence of several NPQ components, chlorophyll and carotenoid pigments in the LHCII-antennae are ultimately responsible for the thermal dissipation of energy during NPQ, but the exact biophysical mechanism remains elusive (Holleboom & Walla, 2014).

The fastest component of NPQ (qE) is induced when the thylakoid protein PsbS is protonated as a result of an increase in ΔpH across the thylakoid membrane (Krause et al. 1982, Li et al. 2000). In addition to PsbS, induction of qE requires the presence of the xanthophyll pigment zeaxanthin (Johnson & Ruban, 2011; Sylak-Glassman et al., 2014). qE occurs in the timescale of seconds to minutes and results

in conformational changes in the PSII-LHCII complex that enable excitation energy dissipation (Betterle et al., 2009). Zeaxanthin is also required for the induction of the qZ component of NPQ, that activates and relaxes in the timescale of minutes to tens of minutes (Dall'Osto et al., 2005; Nilkens et al., 2010). Contrary to qE, qZ does not depend on ΔpH or PsbS.

The slowest component of NPQ is termed qI for photoinhibitory (or sustained) quenching, and it occurs in the timescale of hours or longer. Broadly speaking, qI is a light-induced decrease in the yield of photosynthetic carbon fixation, which can result from several processes. Traditionally, qI has been attributed to the light-induced inactivation and degradation of the PSII reaction centre protein D1 (PSII photoinhibition, discussed in the section 1.4.3). However, sustained NPQ can also results from the plastid lipocalin (LCNP) -dependent quenching that takes place in the PSII antenna, but does not depend on ΔpH, PsbS or zeaxanthin produced by violaxanthin-de-epoxidase (Malnoë et al., 2018). For clarity, it has been suggested to call the LCNP-dependent component of NPQ qH, to distinguish it from NPQ occurring due to PSII photoinhibition. Further adding to the complexity of sustained NPQ, qZ can also contribute to qI (Malnoe 2018). It has also been suggested that inactivated PSI can dissipate excess excitation energy as heat ("PSI-NPQ") (Tiwari et al., 2016).

All of the NPQ mechanisms described above dissipate excess excitation energy as heat. However, a decrease in chlorophyll fluorescence generated by LHCII can also be observed as a result of state transitions (discussed in section 1.4.1) that do not generate heat. The state transition component of NPQ is termed qT. Other processes that lead to decreased chlorophyll fluorescence in plants are chloroplast movement that leads to shading (Cazzaniga et al., 2013), thus decreasing the amount of harvested excitation energy, and possible excitation energy spill-over from PSII to PSI (Kowalczyk et al., 2013).

1.4.3 PSII photoinhibition-repair cycle

Production of oxygen by the OEC inevitably exposes PSII to oxidative damage in light. Especially prone to ROS-induced damage is the reaction centre protein D1 of PSII. Oxidative damage to D1 inhibits PSII activity and the protein must be degraded and replaced by a newly-synthesised one in a process called the PSII photoinhibition-repair cycle, before PSII can regain its function (Aro et al., 1993; Demmig-Adams & Adams, 1992). Although the PSII photoinhibition-repair cycle takes place in all light intensities, inhibited PSII complexes accumulate only in high light intensities, when the rate of photoinhibition exceeds the PSII repair rate (Tyystjärvi & Aro, 1996).

In addition to causing damage to PSII, high light intensities induce the phosphorylation of PSII core proteins D1, D1 and CP43 by the STN8 kinase (Bonardi et al., 2005; Vainonen et al., 2005). Phosphorylation of PSII core is believed to change the interaction between PSII and LHCII and be a prerequisite for PSII repair in high light (Fristedt et al., 2009; Tikkanen et al., 2008). Photoinhibited phosphorylated PSII dimers accumulate in the grana, where the machinery required for the repair of damaged PSII cannot access them (Lindahl et al., 1996; Lu et al., 2011; Suorsa et al., 2014; Yamamoto et al., 1981). Damaged PSII dimers thus migrate to the grana margins, where they are dephosphorylated by the phosphatase PBCP and monomerized (Baena-González et al., 1999; Rintamäki et al., 1996; Rokka et al., 2005; Samol et al., 2012). The damaged D1 protein is then degraded by the FTSH and DegP proteases and replaced by a newly synthesised D1 in stroma thylakoids (Haußühl et al., 2001; Kanervo et al., 2003; Lindahl et al., 1996; L. Zhang et al., 1999). PSII monomers are partially disassembled during D1 degradation and de-novo synthesis, and are reassembled before they migrate back to the grana thylakoids (Aro et al., 2005; Baena-González et al., 1999; Rokka et al., 2005). PSII repair cycle is completed by the dimerization of PSII and assembly of active PSII-LHCII complexes in the grana (Aro et al., 2005).

Traditionally PSII photoinhibition has been viewed simply as an unavoidable consequence of photosynthesis that has been assumed to inevitably limit plant growth. However, the PSII photoinhibition-repair cycle is a tightly regulated process that has increasingly been implicated as a photoprotective mechanism rather than mere photodamage. Adams et al. (2013) have suggested that PSII photoinhibition is a way to decrease photosynthetic activity when the production of sugars is greater than the needs of the plant or when the capacity of the chloroplast to assimilate carbon dioxide into sugars is exceeded. Additionally, PSII photoinhibition has been shown to protect PSI, that lacks a repair machinery, from damage by limiting electron transfer from PSII to PSI (Tikkanen et al., 2014) .

1.4.4 Other regulatory mechanisms

Because PSI does not have a dedicated repair machinery like PSII, oxidative damage to PSI leads to irreversible inhibition of the complex that can be alleviated only by the synthesis of a new PSI supercomplex. To avoid this costly consequence, many photosynthetic regulatory mechanisms protect PSI from over-reduction that can lead to damage caused by superoxide formation. In addition to state transitions and PSII photoinhibition-repair cycle that respectively protect PSI directly or indirectly, also photosynthetic control at the $Cytb_6f$ complex and CET serve a PSI protective function. Photosynthetic control at the $Cytb_6f$ complex slows down the flow of electrons to PSI in excess light and is activated when $Cytb_6f$ is protonated as a result

of increased ΔpH (for a detailed review on $Cytb_6f$ the reader is referred to Malone et al. (2021). CET (introduced in section 1.2.2), on the other hand, functions as a regulatory mechanism as it contributes to the formation of ΔpH and thus the induction of photosynthetic control at $Cytb_6f$ and NPQ (Munekage et al., 2002, 2004; Suorsa et al., 2012). Additionally, adjustment of the ATP/NADPH ratio according to the metabolic cues downstream of the light reactions prevents the over-reduction of the stroma, further protecting PSI (Munekage et al., 2002, 2004; Suorsa et al., 2012).

During abiotic stress conditions, another safety valve is able to protect the plastoquinol pool from over-reduction independently from the $Cytb_6f$. Plastid terminal oxidase (PTOX) oxidizes plastoquinol to reduce O_2 to H_2O in a process called chlororespiration (Carol et al., 1999). Under standard growth conditions PTOX accumulates to a very low level in Arabidopsis, but its amount has been found to increase upon abiotic stress in several plant species (Ivanov et al., 2012; Lennon et al., 2003; Stepien & Johnson, 2018).

1.5 Acetylation in the chloroplast

Surviving in a dynamic environment requires rapid adjustment of enzyme activity, which is often achieved via post-translational modification (PTM) of proteins. Photosynthetic reactions are no exception, and PTMs such as phosphorylation, protonation and thioredoxin-mediated redox regulation have been shown to regulate many crucial steps of both light and carbon assimilation reactions (see sections 1.3.1 and 1.4). In addition to these well studied PTMs, acetylation has recently emerged as a prominent PTM among the chloroplast proteins. While acetylation was first discovered in histone proteins, development of mass spectrometry methods has allowed more sensitive detection of protein acetylation in all subcellular compartments.

Protein acetylation can be divided into two types, based on its location on a protein. N-terminal acetylation, as the name suggests, takes place on the free α-amino group at the N-terminus of a protein and thus can occur on any amino acid residue. N-terminal acetylation often occurs co-translationally and is considered irreversible (Drazic et al., 2016). The second type of protein acetylation is Lys-acetylation, where an acetyl group is attached to the ε-amino group of an internal lysine residue. Unlike N-terminal acetylation, Lys-acetylation is reversible (Drazic et al., 2016). In both types of protein acetylation acetyl coenzyme A (acetyl-CoA) functions as the acetyl group donor and the addition of an acetyl group results in the neutralization of the positive charge of the amino group (Drazic et al., 2016).

After the initial discovery of Lys-acetylation in the chloroplast, mass spectrometry analyses have revealed the presence of around 1000 N-terminally and

Lys-acetylated proteins in leaf samples of Arabidopsis (Bienvenut et al., 2012; Finkemeier et al., 2011; Hartl et al., 2017; Wu et al., 2011; Zybailov et al., 2008). Out of the N-terminally acetylated proteins, roughly 30 % were predicted to localize in the chloroplast, while the same was true for 43% of Lys-acetylated proteins (Bienvenut et al., 2012; Hartl et al., 2017). Based on functional annotation analysis of the identified Lys-acetylated proteins, proteins involved in photosynthesis were one of the most overrepresented groups (Hartl et al., 2017). Indeed, all complexes catalysing the light reactions as well as carbon assimilation were found to be Lys-acetylated. A similar high prevalence of Lys-acetylated proteins in the chloroplast has also been observed in studies on rice and wheat that also show an enrichment of Lys-acetylation in proteins involved in photosynthesis and carbon metabolism (Xiong et al., 2016; Xue et al., 2018; Y. Zhang et al., 2016).

1.5.1 The physiological effect of acetylation on photosynthetic proteins

The high occurrence of acetylation in the chloroplast, and more specifically in photosynthetic proteins, suggests that acetylation might play an important role in photosynthesis. Some support for this hypothesis has been obtained when studying Rubisco, the most heavily Lys-acetylated protein in the chloroplast. In a study by Finkemeier et al. (2011) Rubisco activity was found to increase upon deacetylation of Lys-residues with a human deacetylase enzyme hSIRT3. Similarly, non-enzymatic Lys-acetylation of Rubisco was shown to decrease its activity in a study by Gao et al. (2016). Interestingly, a more recent study showed an increase in Rubisco activation state in the Arabidopsis deacetylase mutant *hda14* that has increased Lys-acetylation of both Rubisco and RCA (Hartl et al., 2017). Lys-acetylation of the RCA was shown to decrease its sensitivity to inhibition by ADP and was suggested to be behind the observed increase in Rubisco activation. The discrepancy between these results may be explained by the fact that different Lys-acetylation sites were affected in the different studies. However, the involvement of Lys-acetylation in the regulation of Rubisco has also been challenged by O'Leary et al. (2020) who argue that due to the low stoichiometry of Lys-acetylation events in Rubisco, acetylation is unlikely to have an effect on the overall enzyme activity *in vivo*.

Similarly to Lys-acetylation, N-terminal acetylation has also been implicated in the regulation of photosynthesis by a handful of studies. Most direct evidence was presented in a study by Hoshiyasu et al. (2013), who showed that N-terminal acetylation of the ATPase subunit ε in wild watermelon protects the subunit from degradation under drought stress, where the non-acetylated isoform of ATP ε specifically decreases. Another example of photosynthetic proteins whose N-

terminal acetylation status responds to environmental cues are the (leaf-type) FNR proteins that show increased acetylation under increased illumination (Lehtimäki et al., 2014). The presence of N-terminal acetylation in the PSII reaction center proteins D1 and D2 discovered by Michel et al., (1988) has sparked a lot of speculation, but no link to function has been found so far. More recently, the high occurrence of N-terminal acetylation in the stroma-exposed N-terminal loops of PSII-LHCII supercomplexes has also lead to the suggestion that N-terminal acetylation might be involved in thylakoid stacking (Albanese et al., 2020).

1.5.2 GNAT-acetyltransferases are responsible for acetylation in the chloroplast

Although protein acetylation can in some conditions (high acetyl-CoA concentration combined with high pH) occur non-enzymatically, most acetylation events in the chloroplast are likely catalysed by acetyltransferase enzymes. Based on studies on eukaryotic nuclear and cytosolic acetyltransferase enzymes, it is generally thought that the two types of protein acetylation are catalysed by specific acetyltransferases. All known enzymes responsible for N-terminal acetylation (NAT) belong to the general control non-repressible 5 (GCN5)-related N-acetyltransferase (GNAT) superfamily, while lysine acetyltransferases (KAT) have been identified in the GNAT, MYST and p300/CBP superfamilies (Drazic et al., 2016). Despite the relatively low sequence homology, GNAT enzymes have conserved secondary and tertiary structures that have enabled the identification of GNAT superfamily proteins in species ranging from bacteria to eukaryotes (Rathore et al., 2016; Ud-Din et al., 2016).

The first report on a chloroplast-localized GNAT enzyme identified AtNAA70 (GNAT4) that was shown to possess NAT activity upon heterologous expression of the recombinant AtNAA70 in *E.coli* (Dinh et al., 2015). Additionally, Lys-acetylation was observed on three internal lysine residues of AtNAA70, pointing to auto-KAT activity of the enzyme. A more comprehensive study of chloroplast acetyltransferases was conducted by Bienvenut et al. (2020), who identified ten putative chloroplast GNATs (GNAT1-10) based on *in silico* analysis and confirmed the chloroplast-localization for seven of the GNAT candidates (GNAT1-5, GNAT7 and GNAT10). Notably, GNAT6 was associated with the chloroplast, while GNAT8 and GNAT9 were localized in the cytosol and/or nucleus. The localization results were supported by a Genevestigator analysis of GNAT transcript abundance, that showed that all chloroplast-localized GNATs were mostly expressed in the green tissues, while GNAT6, GNAT8 and GNAT9 transcripts were present throughout the plant.

In addition to a predicted transit peptide, all chloroplast GNATs contain the conserved GNAT structure consisting of 6-7 β-sheets and four α-helices that form domains A-D. Domain A contains the acetyl-CoA binding site, domain B is required for substrate binding, while domains C and D have been suggested to affect protein stability (Ud-Din et al., 2016). Most variation was observed in the N- and C-terminal regions that affect substrate specificity and binding to potential auxiliary proteins. Interestingly, in addition to the conserved acetyl-CoA binding site, GNAT1-4, GNAT7 and GNAT10 contained a secondary acetyl-CoA binding site (Bienvenut et al., 2020).

Heterologous expression of chloroplast GNATs in *E.coli* followed by mass spectrometry analyses of Lys- and N-terminally acetylated proteins revealed that six chloroplast GNATs show specific KAT and relaxed NAT activity. The remaining two chloroplast GNATs (GNAT1 and GNAT3) exhibited only weak KAT/NAT activity in the study. The relaxed substrate specificity of chloroplast GNATs suggests that the enzymes might have some redundancy *in planta*, pointing to the importance of a robust acetylation machinery in the chloroplast (Bienvenut et al., 2020).

1.5.3 GNAT1 and GNAT2 function as metabolite acetyltransferases in melatonin biosynthesis

In addition to their dual KAT/NAT activity, several studies have implicated GNAT1 (SNAT2) and GNAT2 (SNAT1) in melatonin biosynthesis. In plants, melatonin functions as an antioxidant conferring protection against (a)biotic stresses as well as having signalling functions that affect e.g. gene expression and stomatal aperture (Arnao & Hernández-Ruiz 2019). The importance of melatonin in several aspects of plant physiology together with the recent discovery of a melatonin receptor has prompted the discussion about melatonin being an up until now overlooked phytohormone (Wei et al., 2018). Both GNAT1 and GNAT2 were shown to acetylate serotonin and 5-methoxytryptamine (5-MT) in the last steps of melatonin biosynthesis in Arabidopsis (Lee et al., 2014, 2019). Similarly to their different protein substrate specificities, GNAT1 and GNAT2 exhibit distinct enzymatic properties as metabolite acetyltransferases. While serotonin is the preferred substrate of GNAT1, GNAT2 is more efficient in 5-MT acetylation (Lee et al., 2014, 2019). Both enzymes are inhibited by 5-MT, but GNAT1 activity is also inhibited by melatonin and GNAT2 by serotonin (Lee et al., 2014, 2019).

Interestingly, in Arabidopsis, *gnat1* and *gnat2* mutants accumulate Wt-levels of melatonin in leaves under standard growth conditions, although a decrease in melatonin content was observed in *gnat1* flowers (Lee et al., 2019). While melatonin levels increased in wild type plants after the plants were challenged with an avirulent

pathogen or high light, such an increase was absent in *gnat2* (Lee et al., 2015; Lee & Back, 2018). In both treatments, the decreased melatonin accumulation was accompanied by increased susceptibility of the *gnat2* mutant to the (a)biotic stress in question, suggesting that GNAT2-dependent melatonin production is involved in stress tolerance. Similar results were obtained in studies on GNAT homologues in rice (SNAT1 and SNAT2) that revealed decreased accumulation of melatonin, retarded growth and increased susceptibility to abiotic stress in the *snat1* and *snat2* mutants (Byeon & Back, 2016; Hwang & Back, 2020).

2 Aims of the study

Post-translational modifications of proteins such as phosphorylation, protonation and redox regulation of disulfide bonds have been shown to play pivotal roles in the regulation of photosynthesis. However, the study of these small modifications has long been hindered by methodological limitations. In recent years, advances in mass spectrometry methods have enabled the identification of a myriad of PTMs affecting proteins in all subcellular compartments. Especially interesting is the high prevalence of protein acetylation in the chloroplast, and more specifically in photosynthetic proteins. The presence of several plastid-localized GNAT acetyltransferases highlights the importance of this PTM in the chloroplast. The aim of my PhD project was to shed more light on the role of chloroplast acetyltransferases in chloroplast metabolism with the focus on photosynthesis. More specifically, my aims were:

I) Identify the plastid GNATs involved in the regulation of photosynthesis. (Publications I and III)

II) Elucidate which regulatory processes are affected by protein acetylation and how. (Publications I and II)

III) Find out what other metabolic processes are affected in the *gnat* knock-out mutants. (Publication III)

IV) Elucidate the role of two unknown chloroplast proteins Lys-acetylated by GNAT2. (Publication IV)

3 Materials and Methods

3.1 Plant material and growth conditions

The model plant species *Arabidopsis thaliana,* Columbia-0 accession was used in all publications. Wild-type (Col-0) and mutant plants were grown on a 2:1 peat-vermiculite mix in short day conditions (8 h light/16 h dark) at the photosynthetic photon flux density of 100-130 µmol m^{-2} s^{-1}, as indicated in the publications. Osram Powerstar HQI®-BT 400 W/D PRO Daylight lamps were used as the light source and the growth chamber was kept at +23 °C and 50% relative humidity. For most experiments, mature rosettes of plants grown for 4-5 week were used. To produce seeds, plants were grown in long day conditions at 16 h light/8 h dark.

3.1.1 Screening of knock-out mutants and generation of double mutants

The mutant lines used in the publications (*gnat1, gnat2-1, gnat2-2, gnat4, gnat6, gnat7, gnat10, alm-a* and *alm-b*) were obtained from the European Arabidopsis Stock Centre (NASC) (Scholl et al. 2000). To confirm the presence of the interrupting T-DNA insert in the target gene, genomic DNA from the mutant lines was PCR-amplified using primers binding to both sides of the T-DNA insertion site or the T-DNA insertion and the mutated gene. Two distinct methods were used to estimate transcript abundance of the target gene products: end-point RT-PCR and real time quantitative PCR (Publications I and III). Prior to both analysis methods, RNA was extracted from mature rosettes and treated with a DNAse enzyme to remove contaminant DNA. The purified RNA was used for cDNA synthesis with the iScript™ cDNA synthesis kit (Bio-Rad). The obtained cDNA was used as the template for end-point PCR or real time quantitative PCR performed with the IQ SYBR Green Supermix and the IQ™5 Cycler (Bio-Rad). Details of the PCR analyses are described in Publications I and III.

Double *alm-a/b* lines were produced by crossing single *alm-a* and *alm-b* T-DNA mutant lines. To ensure that the double mutant lines were homozygous, at least three generations of progeny were PCR screened. The *stn7* mutant line was provided by

Mikko Tikkanen (Tikkanen et al., 2006) and the *kea-d* line by Hans-Henning Kunz (Kunz et al., 2014).

3.2 Gel-based protein analyses

3.2.1 Protein isolation and chlorophyll determination

Thylakoid proteins were isolated from fresh mature rosettes that were gently ground in cold isotonic buffer and filtered to remove unground material. The filtrate was resuspended in hypotonic buffer to rupture the chloroplast, followed by centrifugation and resuspension in isotonic storage buffer. All steps were performed in the cold and dark to avoid degradation and phosphorylation of proteins, while dephosphorylation was inhibited by the addition of sodium fluoride to all isolation buffers. Thylakoid samples were frozen in liquid nitrogen and stored at -80 °C. Details of thylakoid protein isolation are described in Publications I-IV.

For total protein isolation, frozen leaf material was homogenized and suspended in a denaturating buffer, followed by an incubation at +68˚C for 10 minutes. Samples were then centrifuged and the supernatant was stored at -80 °C.

The chlorophyll content of thylakoid and total protein samples was determined as described in Porra et al. (1989).

3.2.2 Thylakoid sub-fractionation using digitonin

To assess the relative amount of the appressed thylakoid grana and the non-appressed thylakoid domains (grana margins and stroma lamellae), the thylakoids were sub-fractionated with the mild non-ionic detergent digitonin. Due to its bulky structure, digitonin preferentially solubilizes the non-appressed thylakoid domains that can then be separated from the appressed structures by centrifugation. Determining the amount of chlorophyll *a* and *b*, and their ratio (Porra et al., 1989) in the two sub-fractions enables the indirect assessment of thylakoid structure (Publication II). Additionally, the sub-fractions were used to determine the distribution of proteins in the different thylakoid domains in Publication IV.

3.2.3 Gel electrophoresis, immunoblotting and staining

Thylakoid and total protein samples were solubilized with Laemmli buffer (Laemmli, 1970) supplemented with urea and separated using denaturating gel electrophoresis. For immunoblot analysis, the proteins were then transferred onto a PVDF-membrane and incubated with specific antibodies. The antibody signal was detected either using a horseradish peroxidase-labelled secondary antibody and a

substrate for enhanced chemiluminescence or a secondary antibody labelled with infrared fluorescent dye and the Licor Odyssey CLx imaging system.

Staining of 1D and 2D protein gels was performed using the SYPRO Ruby protein gel stain (Invitrogen) and Pro-Q™ Diamond gel stain (Invitrogen) to visualize total proteins and phosphoproteins, respectively. The stains were used according to the manufacturer's instructions.

3.2.4 Native gel electrophoresis

Thylakoid samples were solubilized with weak non-ionic detergents β-dodecyl maltoside or digitonin to maintain their native structure, while gently isolating them from the surrounding thylakoid membrane. To facilitate separation, the solubilized samples were supplemented with Coomassie-250 dye or sodium deoxycholate that add a negative charge to the samples and separated using large pore native gel electrophoresis (Järvi et al., 2011). In addition to scanning, the clear native gels (without the Coomasie-250 dye) were also imaged with the Licor Odyssey CLx system to visualize chlorophyll fluorescence (Publication IV).

For denaturating 2D gel electrophoresis, strips from native gels were solubilized with Laemmli buffer (Laemmli 1970) and separated using denaturating gel electrophoresis to resolve the distinct subunits comprising the photosynthetic complexes. For native 2D gels (Publication II) digitonin-solubilized thylakoids were separated using native gel electrophoresis followed by solubilization with β-dodecyl maltoside and separation on second dimension as described in Rantala et al. (2017). To visualize the proteins, the 2D gels were immunoblotted or stained as described above.

3.3 Determination of photosynthetic activity

3.3.1 Chlorophyll fluorescence and P700 measurements

To assess the function of the photosynthetic electron transfer chain *in vivo*, chlorophyll *a* fluorescence and P700 difference absorption (830-875 nm) were measured using Dual-PAM 100 (Walz). The light curve measurements (Publications I, III and IV) were performed on dark- adapted plants that were subjected to intervals of increasing light intensity, followed by a saturating pulse to determine the quantum yields of PSI and PSII and calculate their *in vivo* parameters. In Publication I, state transition measurements were performed using the PAM-101 fluorometer (Walz) by illuminating dark-adapted plants with blue and far-red light.

Additionally, the fluorescence emission spectra were measured at 77K to assess the relative fluorescence emission from PSII (peaks at 685 and 695 nm), PSI (peak

at 735 nm) and detached LHCII (peak at 680 nm). The emission spectra were recorded from isolated thylakoids (Publication I).

3.3.2 Electrochromic shift measurements

To evaluate the magnitude and partitioning of proton motive force (*pmf*) in the *gnat* mutants (Publication III), the light-induced absorbance difference between 550 and 515 nm (ECS) was measured using a DUAL-PAM-100 (Walz) spectrometer equipped with the P515/535 accessory module (Schreiber & Klughammer, 2008). The measurements were performed on whole dark-adapted plants and the results were used to determine the partitioning of *pmf* to ΔpH and ΔΨ and the proton flux (vH^+) and conductivity (gH^+).

3.3.3 Carbon assimilation measurements

Carbon assimilation of intact plants (Publication III) was evaluated by measuring CO_2 assimilation and H_2O evaporation with the GFS-3000 gas exchange system (Walz) at different light intensities and different CO_2 concentrations.

3.3.4 Photoinhibition experiments

To study PSII photoinhibition (Publication III), detached leaves were floated in water or water supplemented with 2.3 mM lincomycin, inhibitor of chloroplast protein synthesis, for 16 h to allow proper infiltration. The leaves were then subjected to a high light treatment of 600-1000 µmol photons m^{-2} s^{-1} for 2 h. The high light treatment was followed by a recovery period in growth light conditions. The yield of PSII was assessed prior and during the high light treatment as well as during recovery by measuring the Fv/Fm value with FluorPen (Photon Systems Instruments). Leaf material for total protein isolation was collected to evaluate the effect of the photoinhibition treatment on the amount of D1 protein using immunoblot analysis.

3.3.5 Pigment analyses

Total chlorophyll content in leaves was determined by incubating weighed leaf discs in N,N-dimethylformamide in darkness. The extract was then used for absorbance measurements at 646.6, 663.6 and 750 nm and the obtained values were used to calculate the total chlorophyll content (Inskeep and Bloom 1985) (Publication III).

For the determination of xanthophyll cycle pigments (zeaxanthin, violaxanthin and antheraxanthin), leaf material was frozen and ground, and the pigments were

extracted with methanol. The pigment extracts were then analysed with HPLC as described in Gilmore and Yamamoto (1991) (Publication III).

3.4 Analyses of Lys-acetylation

3.4.1 Recombinant protein work and Lys-acetyltransferase activity assay

Recombinant His-tagged GNAT2 for *in vitro* Lys acetylation assay was cloned and purified by Prof. Iris Finkemeier's group at the University of Münster (Publication I). To measure the Lys acetyltransferase activity of GNAT2, the purified recombinant protein was incubated with acetyl-CoA and a synthetic peptide substrate coupled to anthranilic acid that can be detected at 360 nm. Samples collected after the incubation were separated using reverse phase HPLC coupled to a 360 nm detector.

3.4.2 Quantitative Lys-acetylome and whole proteome analyses

The quantitative Lys-acetylomes and whole proteomes of Col-0 and *gnat2* plants were determined using stable dimethyl labelling of trypsin-digested peptides isolated from frozen leaf material. For Lys-acetylome analysis, the labelled peptides were enriched using immunoaffinity chromatography with an acetyl-Lys antibody. The peptides for both analyses were fractionated with reverse phase HPLC and subjected to mass spectrometry analysis using the Q Exactive HF mass spectrometer. The details of mass spectrometry data acquisition and analysis are described in Publication I.

3.5 Microscopy

To determine the localization of GNAT2 *in planta*, Arabidopsis protoplasts were transformed with a pFF19-GNAT2:YFP plasmid expressing N-terminally tagged GNAT2-YFP and imaged using confocal fluorescence microscopy (Publication I). YFP fluorescence was excited at 514 nm and detected using a 560-615 nm band-pass filter, while chlorophyll fluorescence was excited at 488 nm and detected within 647-745 nm. To verify the chloroplast-localization of GNAT2-YFP, the YFP signal was compared to localization marker proteins in the chloroplast (NAA70-YFP), the cytosol (RFP) and plasma membrane (TMD23-RFP).

The ultrastructure of the thylakoid membranes of Col-0 and *gnat2* plants was studied using transmission electron microscopy (Publication I). For each genotype,

leaf samples of seven biological replicates were analysed and in total, membrane layers and grana heights were quantified from 700 grana stacks per genotype.

3.6 Circular dichroism spectroscopy

The macro-organization of the thylakoid membranes of Col-0, *gnat2* and *stn7* plants were analysed using circular dichroism (CD) spectroscopy (Publication II). The CD spectra were measured from intact leaves and thylakoid membranes at room temperature in the spectral range of 400-800 nm and normalized to the absorption maxima at 680 nm. The CD spectroscopy measurements were performed in Bettina Ughy's group at the University of Szeged.

3.7 Metabolomics

The metabolomes of Col-0 and the *gnat* mutants (Publication III) were determined using a non-targeted metabolomic approach by Afekta Technologies (Finland). Briefly, the metabolites were extracted from homogenized leaf material with methanol and the extracts were analysed using UHPLC-MS. A similar approach was used to determine the melatonin content in Col-0 and *gnat2* leaf samples in the Viikki Metabolomics Unit at the Metabo-HiLIFE platform (University of Helsinki).

3.8 *In silico* analyses

3.8.1 ALM gene expression and sequence analyses

The expression of *ALM* genes was analysed with the Genevestigator tool (Hruz et al., 2008) using publicly available expression data. For the sequence analysis of ALM proteins, ALM homologues from different species were identified using the BLASTp tool (Altschul et al., 1990) against selected proteomes from the Phytozome database (plant species) (Goodstein et al., 2012), UniProtKB (cyanobacteria) and the NCBI non-redundantprotein sequences database (other taxonomic groups). The ALM sequences were aligned using the MUSCLE algorithm (Edgar, 2004) in the Jalview software (Waterhouse et al., 2009).

3.8.2 Structural modelling

In silico modelling of ALM-A structure and its potential interaction with the M-LHC trimer was performed by Serhii Vakal and Tiina Salminen (Structural Bioinformatics Laboratory and InFLAMES Research Flagship Center, Åbo Akademi University). To predict the potential signal peptides, cleavage sites, transmembrane regions and

the topology of the protein, the ALM-A amino acid sequence was analysed using PrediSi (Hiller et al., 2004) TOPCONS (Tsirigos et al., 2015), and Phobius (Madeira et al., 2022). The structure of ALM-A was modelled with AlphaFold2 (Mirdita et al., 2022) and visualized with The PyMOL Molecular Graphics System.

For the ALM-A and M-LHCII interaction analysis, the M-LHCII pentamer and the Lhcb1/Lhcb3 trimer were isolated from the X-ray crystal structure of the PSII supercomplex (PDB ID 7OUI). The details of the structural modelling are described in Publication IV.

4 Results

4.1 GNAT2 is a chloroplast-localized Lys-acetyltransferase

To gain insight into the role of protein acetylation in the chloroplast, we studied the GNAT2 (NSI, SNAT1) enzyme that contains a predicted acetyltransferase domain as well as a transit peptide targeting it to the chloroplast (Publication I). To confirm the chloroplast-localization of GNAT2, Arabidopsis protoplasts were transformed with a vector transiently expressing GNAT2 tagged with a yellow fluorescent protein (GNAT2-YFP). Confocal microscopy of the protoplasts revealed colocalization of the YFP signal with chlorophyll autofluorescence, with no YFP fluorescence detected in other subcellular compartments (Publication I: Figure 1). Immunoblot analysis of chloroplast fractions isolated from transgenic Arabidopsis plants expressing GNAT2-YFP further showed that GNAT2 is present in the soluble fraction. These results support the findings of Lee et al. (2014) and confirm that GNAT2 is chloroplast-localized.

Lys-acetyltransferase activity of GNAT2 was investigated *in vitro* by producing a recombinant GNAT2 enzyme that was used to catalyse Lys-acetylation of a synthetic peptide substrate in the presence of acetyl-CoA. Indeed, HPLC analysis of the reaction products revealed the accumulation of a Lys-acetylated peptide in the samples containing recombinant GNAT2 (Publication I: Figure 1). Further evidence of GNAT2 functioning as an active Lys-acetyltransferase *in planta* was obtained with quantitative mass spectrometry analysis of *gnat2* mutant and Col-0 Lys-acetylomes. Based on our analysis, Lys-acetylation levels of several chloroplast proteins were significantly decreased in the *gnat2* samples as compared to Col-0, indicating that GNAT2 has multiple potential Lys-acetylation targets in Arabidopsis (**Table 1**, Publication I: Figure 2). Most of the identified Lys-acetylation targets of GNAT2 were stroma-localized or -exposed, but an interesting exception was found in the form of the lumenal PSBP-1 protein. A possible explanation to this is that while GNAT2 most likely functions in the stroma, PSBP-1 could be acetylated prior to its transport into the lumen. However, some proteins also exhibited increased Lys-acetylation in the *gnat2* mutants, suggesting the existence of interplay between Lys-acetylation of different proteins as well as the presence of other active

acetyltransferases in the chloroplast. Lys-acetylation was also increased in a few cytosolic proteins in *gnat2*, while the overall accumulation of chloroplast and cytosolic proteins was largely unchanged as compared to Col-0.

Table 1. Proteins with changed Lys-acetylation status in the *gnat2* mutants identified using quantitative Lys-acetylome analysis. Lys-acetylation sites with $\log_2$ fold changes ≥0.5 or ≤−0.5 ($\log_2$ fold change values are negative when the fold change is < 1) and false discovery rate corrected P value ≤ 0.05 (LIMMA) are presented as well as two sites potentially involved in state transitions (LHCB1.4 and PSAH1/2). Only chloroplast-localized proteins are included in the table.

PROTEIN	AGI-CODE	LYS-ACETYLATION SITE	LOG_2 FOLD CHANGE
KEA1/2	At1g01790/At4g00630	K168/K170	-5.37
Unkown protein (ALM-A/ALM-B, Publication IV)	At2g05310/At4g13500	K62	-2.29
PSBP-1	At1g06680	K88	-3.70
FER1	At5g01600	K134	-0.62
LHCB1.4	At2g34430	K40	-0.30
PSAH1/2	At3g16140/At1g52230	K138	-0.28
LHCB6	At1g15820	K220	0.69
Plastid-lipid associated protein PAP	At3g26070	K225	0.96
ATPF	AtCg00130	K119	0.57
SOUL heme binding family protein	At5g20140	K320	0.81
SBPASE	At3g55800	K307	0.56
ENH1	At5g17170	K233	0.53

4.2 GNAT2 is required for state transitions

The first clues of the involvement of GNAT2 in the regulation of photosynthesis were obtained when the thylakoid protein complexes isolated from *gnat2* mutants were analysed using blue native gel electrophoresis. Solubilization of thylakoid protein complexes with the mild detergent digitonin preserves the labile interactions between the proteins, thus allowing the separation of intact supercomplexes (Järvi et al., 2011). Intriguingly, blue native gel analysis of digitonin-solubilized thylakoid samples revealed that the *gnat2* mutants fail to accumulate the PSI-LHCII supercomplex, also referred to as the "state transition" complex (Kouřil et al., 2005; Pesaresi et al., 2009) (Publication I; Figure 3). The PSI-LHCII supercomplex usually

accumulates in low and moderate light intensities (Pesaresi et al., 2009), and was observed in Col-0 thylakoids isolated from growth light conditions, but was absent in the *gnat2* samples. As revealed by our blue native gel analysis, the pattern of the thylakoid protein complexes of *gnat2* thylakoids closely resembled that of the *stn7* mutant, which lacks the STN7 kinase regulating state transitions (Bellaflore et al., 2005).

The lack of state transitions in the *gnat2* mutants was also observed by measuring the 77K fluorescence emission spectra of thylakoids isolated from growth and red light conditions that induce the formation of the PSI-LHCII supercomplex. In these conditions, the fluorescence emission peak at 735 nm, originating from PSI, was significantly lower in the *gnat2* samples (Publication I: Figure 4). No differences in the 77K emission spectra were observed in thylakoids isolated from dark and far-red light conditions that favour the dissociation of PSI-LHCII. Pulse amplitude modulated chlorophyll fluorescence measurements of intact leaves confirmed the inability of *gnat2* lines to perform state transitions as evidenced by increased steady-state and maximal chlorophyll fluorescence in light conditions favouring PSII.

Based on the Lys-acetylome analysis of the *gnat2* mutants, several Lys-acetylation targets of GNAT2 could potentially affect state transitions. Such targets include the OEC protein PsbP-1 (AT1G06680), LHCII antenna protein Lhcb1.4 (AT2G34430) and PSI LHCII docking site proteins PsaH-1/2 (AT3G16140; AT1G52230). Additionally, we analysed the composition and Lys-acetylation sites of the LHCII trimer and PSI-LHCII complexes separated using blue native gel electrophoresis. While no differences were observed in the composition of the LHCII trimers when comparing *gnat2, stn7* and Col-0, Lys-acetylation of Lhcb2.2 was not detected in *gnat2-1* and was present in only one biological replicate of *gnat2-2*. In contrast, Lhcb2.2 Lys-acetylation was detected in two to three biological replicates of *stn7* and Col-0 samples. Mass spectrometry analysis of the PSI-LHCII complex from Col-0 samples revealed the presence of Lys-acetylated Lhcb1.2, Lhcb1.5 and PsaH. Unfortunately, the acetylation targets of GNAT2 identified earlier, were not detected in the analysis of the PSI-LHCII complex, likely due to the lack of an immunoaffinity enrichment step in the latter.

4.3 The thylakoid dynamics are impaired in *gnat2*

Phosphorylation of LHCII, and more specifically Lhcb2, is a prerequisite for state transitions and has been shown to regulate thylakoid dynamics by affecting the rearrangement of the thylakoid protein complexes (Kyle et al., 1983; Pietrzykowska et al., 2014; Wood et al., 2019). This, together with the similar state transition phenotype of *gnat2* and *stn7* mutants prompted us to examine protein phosphorylation in the *gnat2* lines. Surprisingly, immunoblot analysis using an

antibody against phosphorylated threonine (and serine) revealed no significant difference in the phosphorylation of LHCII and PSII core proteins between the *gnat2* lines and Col-0 (Publication I: Figure 5). Similarly, no deficiency in phosphorylation was detected in the *gnat2* samples probed with specific antibodies against phosphorylated Lhcb1 and Lhcb2, but rather the phosphorylation of these proteins was increased in the mutants (Publication I: Figure 5; Publication II: Figure 1). An increase in LHCII phosphorylation in *gnat2* was also detected with Pro-Q™ Diamond gel stain binding specifically to phosphoproteins (Publication III; Figure 3). Together these results show that *gnat2* mutants are not deficient in LHCII phosphorylation, unlike *stn7* that lacks it completely, suggesting that LHCII phosphorylation is not the only determinant of state transitions.

To further dissect the phosphorylation in the *gnat2* mutant, the distribution of phosphorylated Lhcb1 and Lhcb2 was investigated using 2D blue native gels. Thylakoids were first solubilized with digitonin to maintain the labile interactions between the complexes, followed by solubilization with a slightly stronger detergent, β-dodecyl maltoside, to (partly) detach LHCII from the PS-complexes (Publication II; Rantala et al., 2017). The resulting 2D blue native gels allow to separate the different pools of LHCIIs, namely the dissociated M-LHCII and L-LHCII as well as the LHCII still attached to the PSII supercomplexes. In both Col-0 and *gnat2* samples, pLhcb1 was similarly distributed in disconnected M-LHCII and L-LHCII and in the PSII-LHCII supercomplexes (Publication II: Figure 3). However, there were marked differences in the distribution of pLhcb2. In Col-0, pLhcb2 was found predominantly in the L-LHCII, although some signal was also observed in the PSII-LHCII-PSI supercomplexes that also contain some L-LHCII. In *gnat2*, on the contrary, pLhcb2 was present in all pools of LHCII, including M-LHCII, which is usually depleted of Lhcb2. The presence of Lhcb2 in the M-LHCII complex was confirmed using an antibody against unphosphoryated Lhcb2.

One of the consequences of LHCII phosphorylation has been shown to be the loosening of thylakoid ultrastructure, which is thought to decrease lateral heterogeneity of the photosynthetic complexes, thus enabling state transitions (Wood et al., 2018, 2019). The increase in LHCII phosphorylation and altered distribution of P-Lhcb2 in *gnat2* lead us to investigate the structure and dynamics of the thylakoid membranes in more detail. Transmission electron microscopy revealed that the *gnat2* mutants exhibited more compact packing of grana stacks when compared to Col-0 (Publication I: Figure 3). Additionally, the macro-organization of the thylakoid membranes of *gnat2* and *stn7* leaves and isolated thylakoids were compared to Col-0 using circular dichroism (CD) spectroscopy. In the mutants, the psi-type CD bands at (+)690 nm, (-)674 nm and (+)506 nm were diminished indicating changes in LHCII composition and a decrease in LHCII trimers or decreased PSII-LHCII complex stability (Publication II: Figure 2; Tóth et al., 2016). The changes in the CD

spectra were most prominent in isolated thylakoids, that showed decreased amplitude of all three bands mentioned above, while only the band at (+)690 nm was diminished in leaves. The CD spectra results indicate that the organization of the photosynthetic complexes is, similarly to *stn7*, altered in the *gnat2* mutant.

To gain better understanding of the light-induced dynamics of the thylakoid membranes, we used digitonin to subfractionate thylakoids from dark and growth light adapted plants to appressed (grana stacks) and non-appressed fractions (grana margins and stroma lamellae). In the dark, the thylakoid membranes are tightly packed and there is strict lateral heterogeneity of the thylakoid supercomplexes. When plants are exposed to moderate light, LHCII phosphorylation leads to the loosening of grana stacks and decreased lateral heterogeneity (Wood et al., 2019). Thus, in the light there is an increase in the amount of non-appressed regions of the thylakoid membrane that are accessible to solubilization with digitonin. The changes in thylakoid ultrastructure can be assessed indirectly by measuring the chlorophyll content of the digitonin-solubilized fraction.

Intriguigly, *gnat2* thylakoids showed no light-induced dynamics upon shift from dark to growth light, as reflected by only a marginal increase in the amount of chlorophyll *a* and *b* in the non-appresed thylakoid fraction (Publication II: Figure 1). While chlorophyll *a* is bound to PSI and LHCs, the majority of chlorophyll *b* is bound to LHCII, which is mostly restricted to the grana thylakoids in the dark (Andersson & Anderson, 1980). In Col-0 thylakoids, especially the amount of chlorophyll *b* increases upon the shift from dark to growth light, while this increase is very small in *gnat2*. This indicates that the majority of LHCII remains in the appressed fraction in the mutant regardless of the light conditions. Subfractionation of *stn7* thylakoids from the same conditions revealed a very similar decrease in thylakoid dynamics as in *gnat2*, although phosphorylation was not deficient in the latter. In fact, Lhcb1 and Lhcb2 were already more phosphorylated than Col-0 in the dark, and the difference in phosphorylation increased upon the shift to growth light (Publication II: Figure 1).

To study whether the more compact packing of grana and decreased thylakoid dynamics are behind the lack of state transitions in *gnat2*, thylakoids were isolated with and without $MgCl_2$. Mg^{2+} is required for thylakoid stacking and its absence results in the randomization of the thylakoid membrane, thus enabling the interaction of PSI and LHCII (Barber, 1980; Murakami & Packer, 1971). However, the randomization of thylakoid membranes only partially restored PSI-LHCII complex formation in *gnat2*, indicating that other factors also contribute to the lack of state transitions in the mutant (Publication II: Figure 4). Defects in the PSI-LHCII docking site could be inhibiting state transitions, although no changes in the accumulation of the docking site proteins PsaH and Lhca4 were observed in immunoblot analysis of *gnat2* thylakoid samples (Publication I: Figure 5).

4.4 Loss of GNAT2 results in the clearest photosynthetic phenotype among the chloroplast GNATs

In addition to GNAT2, seven other GNAT enzymes show chloroplast-associated localization (Bienvenut et al., 2020). To study the involvement of the chloroplast GNATs in photosynthesis, we subjected six GNAT single knock-out mutants (*gnat1, gnat2, gnat4, gnat6, gnat7, gnat10*) to photosynthetic characterization. While no differences were observed between the visual phenotype of most *gnat* lines and Col-0, *gnat2* plants appeared slightly smaller when grown at the PPFD of 100 µmol m^{-2} s^{-1} (Publication III: Figure 1). The growth retardation of *gnat2* was light dependent and decreased when plants were grown in higher light intensities. Interestingly, no changes in the growth of *gnat2* were observed in Publication I, although the plants were grown in the same 100 µmol m^{-2} s^{-1} photon light intensity as in Publication III, suggesting that changes in the light quality might also contribute to the growth defect of *gnat2*. Total chlorophyll content was also unchanged in all *gnat* mutant lines, but the chlorophyll *a* to *b* ratio was slightly lower in *gnat2* (Publications I and III).

The photosynthetic properties of the *gnat* mutant lines were assessed by measuring light response curves of chlorophyll fluorescence and P700 absorbance using Dual-PAM. Similarly to the unchanged growth phenotype, most *gnat* lines did not differ from Col-0. However, *gnat2* lines exhibited decreased yield of photosystem II (Y(II)) accompanied by an increase in the yield of nonregulated energy dissipation (Y(NO)) and a decrease in photochemical quenching parameters qL and qP in light intensities below growth light (Publications I and III). These results indicate excess excitation of PSII, which is likely caused by the lack of state transitions in the *gnat2* mutants. In light intensities above growth light, *gnat2* exhibited slightly higher NPQ than Col-0. Despite the increase in NPQ in *gnat2*, the mutant showed no changes in the accumulation of the PsbS and VDE proteins required for NPQ induction, nor in the amount of the xanthophyll cycle pigments (Publication III).

Another feature unique to the *gnat2* mutant, was the increased phosphorylation of the LHCII proteins discussed in section 4.3. The changes in phosphorylation that were present also in high light and the decreased dynamics of the *gnat2* thylakoids prompted us to study the PSII photoinhibition-repair cycle in the *gnat2* mutant (Publication III: Figure 3). To this end, detached leaves were challenged with a high light treatment at the PPFD of 600 µmol m^{-2} s^{-1} in the presence and absence of lincomycin to inhibit chloroplast translation and thus block PSII repair. In the presence of lincomycin, the leaves were more susceptible to photoinhibition than the control samples, as monitored by measuring Fv/Fm and the amount of D1 protein throughout the treatment. However, no changes were observed between the *gnat2* and Col-0 samples. In accordance, both *gnat2* and Col-0 leaves (not treated with

lincomycin) showed similar recovery of Fv/Fm and D1 protein levels, when the leaves were moved to growth light after the high light treatment. These results show that the PSII photoinhibition-repair cycle is unaffected in the *gnat2* mutant in the studied conditions.

An interesting feature common to all of the studied *gnat* mutants was the higher accumulation of Rubisco observed when *gnat* thylakoid samples were separated on blue native gels and the gels were stained with Coomassie (Publication III: Figure 2). The result was confirmed by immunoblot analysis of thylakoid samples separated using denaturating gel electrophoresis. No changes in Rubisco were observed in total protein samples, indicating that Rubisco is more tightly associated to the thylakoids in the *gnat* mutants. A similar trend was observed when RCA levels were compared in the thylakoid and total protein samples. However, the increase in the Rubisco and RCA in the thylakoids did not affect the net CO_2 assimilation of the studied *gnat* mutant lines (*gnat1, gnat2* and *gnat10*).

4.5 Chloroplast GNAT mutants have unique metabolic profiles, with some shared features

The involvement of GNAT1 and GNAT2 in melatonin biosynthesis (Lee et al. 2014, 2019) prompted us to investigate the effect of chloroplast GNATs on the metabolome. Untargeted metabolome analysis of GNAT knock-out lines (*gnat1, 2, 4, 7* and *10*) utilizing UHPLC–QTOF–MS revealed that inactivation of specific GNATs affected the abundance of a number of metabolites (Publication III). However, the extent of the metabolome changes depended on the affected GNAT enzyme. Inactivation of GNAT10 resulted in most changes to the metabolome with 89 metabolites up- or downregulated in *gnat10* as compared to Col-0. The mutants *gnat2, gnat4* and *gnat7* showed significant changes in the levels of 28, 46 and 38 metabolites, respectively. Inactivation of GNAT1 had the smallest effect on the metabolome, as the amount of only four metabolites was significantly changed in the *gnat1* mutant compared to Col-0.

Interestingly, the studied *gnat* mutant lines exhibited several shared features in their metabolomes. Defect in almost any chloroplast GNAT (with the exception of GNAT1) resulted in increased levels of the lipids monogalactosyldiacylglycerol (MGDG), diacylglycerol (DG) and lysophosphatidylglycerol (LPG 18:3) (**Table 2**). Similarly, the amount of serine was increased in all studied *gnat* lines. Defect in almost any chloroplast GNAT resulted in reduced levels of the antioxidant ascorbate, several oxylipins and the jasmonic acid (JA) biosynthesis intermediate dinor-12-oxophytodienoic acid (dnOPDA) (**Table 2**).

Table 2. Shared features of the *gnat* mutant metabolomes. Fold changes of the selected metabolites that behave similarly in at least four *gnat* lines (n = 5). Only the fold changes with the FDR-corrected P-value (q-value) of < 0.1 are included in the table (fold changes with q-values < 0.01 are marked in bold). Abbreviations: MGDG, monogalactosyldiacylglycerol; DG, diacylglycerol; LPG, lysophosphatidylglycerol; OxoOTrE, oxo-octadecatrienoic acid; FA, fatty acid; HpOTrE, hydroperoxyoctadecatrienoic acid; EpKODE, epoxy-keto-octadecadienoic acid; dnOPDA, dinor-12-oxophytodienoic acid.

		FOLD CHANGES WITH Q-VALUE OF < 0.1 (<0.01 in bold)				
CURATED ID	**COMPOUND CLASS**	***gnat1* vs Col-0**	***gnat2* vs Col-0**	***gnat4* vs Col-0**	***gnat7* vs Col-0**	***gnat10* vs Col-0**
Serine	Amino acid	**1.69**	1.42	**1.53**	1.35	**1.55**
MGDG(18:3/16:3) (isomer 1)	Glycosyldiradyl-glycerol	-	1.81	**2.08**	**1.96**	**2.12**
MGDG(18:3/16:3) (isomer 2)	Glycosyldiradyl-glycerol	-	1.35	1.42	-	**1.53**
MGDG(18:3/18:3)	Glycosyldiradyl-glycerol	-	-	1.34	1.29	**1.56**
DG(18:3/18:3) (dilinolenin)	Diacylglycerol	-	**1.31**	1.31	-	1.33
LPG(18:3)	Lysophosphatidyl-glycerol	-	**1.47**	1.38	1.39	**1.61**
Ascorbic acid	Vitamin	-	0.27	0.18	0.15	0.19
OxoOTrE (isomer 1)	Oxylipin	-	-	0.68	**0.66**	**0.69**
FA 13:3+1O	Oxylipin	-	0.38	0.36	0.34	0.37
HpOTrE (isomer 3)	Oxylipin	-	0.60	0.59	0.56	0.56
FA 18:4+2O (isomer 1)	Oxylipin	-	0.51	0.60	0.58	0.54
EpKODE (isomer 1)	Oxylipin	-	-	0.74	0.76	0.74
HpOTrE (isomer 2)	Oxylipin	-	0.62	0.67	0.61	0.56
EpKODE (isomer 2)	Oxylipin	-	0.63	-	0.63	0.61
dnOPDA (isomer 1)	Octadecanoid	-	0.60	0.69	0.62	0.57

In addition to the shared metabolome features, inactivation of distinct GNATs also resulted in some specific changes in the metabolomic profiles. The most prominent effect was the marked decrease of two acetylated metabolites: Nα-acetyl-l-arginine decreased in *gnat2* (fold change 0.108) and N-acetylproline in *gnat7* (fold change 0.015). Other noteworthy changes were the increase in the amount of free

amino acids as well as di- and tripeptides in the *gnat10* mutant and the auxin-conjugate indole-3-acetyl-l-alanine in *gnat7*.

Due to its important role in plant physiology as well as the involvement of GNAT1 and GNAT2 in its biosynthesis (Lee et al., 2014, 2019), we were interested to see whether the plastid GNATs have an effect on melatonin biosynthesis. However, the untargeted metabolomic approach failed to detect melatonin or any intermediates of the melatonin biosynthetic pathway. Nevertheless, we used an alternative UPLC–MS approach to detect melatonin in the *gnat2* lines. In line with previous results by Lee and Back (2018), melatonin levels showed no decrease in the *gnat2* mutants, but were slightly increased. These results indicate that GNAT2 is not essential for melatonin production under standard growth conditions.

4.6 Acetylated Little Membrane protein A (ALM-A) and B (ALM-B) bind to M-LHCII and affect the stability of the PSII-LHCII supercomplexes

Among the putative Lys-acetylation targets of GNAT2 identified in Publication I, were two small proteins of unknown function encoded by the genes At2g05310 and At4g13500. A closer look at the two proteins revealed that they are almost identical (including the Lys-acetylated peptide identified in our analysis) and in addition to a predicted transit peptide and a hydrophilic N-terminal region, contain one transmembrane domain. Based on the little knowledge we had of the two proteins, we named them Acetylated Little Membrane protein A (ALM-A, At2g05310) and B (ALM-B, At4g13500).

To gain more insight into the potential function of ALM-A and ALM-B, we utilized bioinformatic tools including gene expression analysis using Genevestigator and a BLASTp search of the Phytozome and the NCBI non-redundant proteins databases (Publication IV). According to the public databases available on Genevestigator, both *ALM* genes are mainly expressed in the green tissues or Arabidopsis and their expression increases as the rosette matures with the exception of the bolting phase, during which the expression decreases (Publication IV: Figure 2). In most studied tissues, the expression of *ALM-A* is somewhat higher than that of *ALM-B*, and *ALM-A* is also expressed in the reproductive tissues where *ALM-B* expression in very low. The BLASTp search further revealed that *ALM* genes are conserved in the green lineage, as *ALM* paralogues were found in green alga and flowering plants (95% occurrence in the Phytozome database), but are absent in cyanobacteria. Interestingly, *ALM* paralogues were a lot less prevalent in gymnosperms and non-seed plants with the occurrence range of 0-50% (Publication IV: Table 1). ALM expression in the green tissues together with its conservation

among photoautotrophic eukaryotes suggests that the proteins have an important function in photosynthesis.

Encouraged by the bioinformatic results, we proceeded to study ALM function *in vivo* using an antibody raised against a peptide common to both ALM-A and ALM-B, and a double *alm-a/b* mutant generated by crossing two T-DNA single mutant lines (SALK_015982 and GABI_209A05). The first direct hint of ALMs involvement in photosynthesis was obtained when we studied the localization of ALMs within the thylakoid protein complexes using 2D-BN-SDS-PAGE followed by immunoblotting. Intriguingly, the ALM signal was detected co-migrating with free M-LHCII, but was absent from the PSII-LHCII supercomplexes that still contain the M-LHCII complex (Publication IV: Figure 4). Support for the potential interaction between ALM and M-LHCII was acquired by structural modelling of the ALM-A protein together with the M-LHCII pentamer complex containing an Lhcb1.4/Lhcb3.1 heterotrimer and monomeric Lhcb4 and Lhcb6 proteins. The structural modelling was done with the assumption that the hydrophilic N-terminal region containing the Lys-acetylation site is exposed to the stroma, where it most likely is accessible for acetylation by GNAT2. Most predictions suggested that the transmembrane domain of ALM-A could bind to the cleft between Lhcb1.4 and the monomeric Lhcb4 and Lhcb6 (Publication IV: Figure 4). Interestingly, the cleft showed high mobility within the M-LHCII complex, suggesting that its availability for binding of ALM may vary. Another noteworthy observation is the high co-occurrence of *ALM* genes together with *LHCB4* that was observed in almost all genomes of non-flowering plants encoding ALM (Publication IV: Table 1).

Analysis of thylakoid protein complexes isolated from *alm-a/b* mutants from growth light and following a 4 h high light treatment revealed a potential physiological consequence of ALMs association with M-LHCII. Clear native gel analysis showed that the lack of the ALM proteins stabilized the PSII-LHCII supercomplexes in both light conditions, but especially under high light (Publication IV: Figure 5). Quantification of the fluorescence signal arising from the PSII-LHCII supercomplexes and the free LHCII (normalized to total fluorescence) after the clear native run revealed that in high light, the *alm-a/b* mutants showed a 26 % increase and 9 % decrease in fluorescence, respectively, when compared to Col-0. Native gel analysis of the *alm-a/b* thylakoid protein complexes revealed no deficiency in the accumulation of the state transition complex, indicating that ALM is not required for state transitions (Publication IV: Figure 5). However, our results suggest that ALM proteins are required to dynamically readjust the PSII antenna size, possibly by facilitating M-LHCII disassociation from the PSII supercomplexes.

5 Discussion

Post-translational modification of proteins has a well-established role in the regulation of photosynthesis. Especially phosphorylation has been implicated in several crucial regulatory processes, such as the balancing of excitation energy distribution via state transitions and the PSII-photoinhibition-repair cycle (see section 1.4). Reversible phosphorylation of the thylakoid proteins (above all LHCII) has been shown to be an important determinant of thylakoid structure and dynamics, likely because of the strong negative charge it introduces to the thylakoid protein complexes that largely dictate the organization of the thylakoid membrane (for review: Johnson & Wientjes, 2020). However, in recent years the development of mass spectrometry methods has enabled the identification of other PTMs, such as acetylation, affecting chloroplast proteins, and opened up new horizons for the study of photosynthesis regulation. In this thesis, I have focused on elucidating the physiological role of a group of newly identified chloroplast GNAT acetyltransferase enzymes with a special focus on photosynthesis (Publications I-III). Our work has shown that GNAT2 is required for state transitions and has a marked effect on thylakoid dynamics (Publications I-II). The remaining chloroplast GNATs investigated in this work (GNAT1, GNAT4, GNAT6, GNAT7 and GNAT10) do not exhibit any clear photosynthetic phenotype, but have a marked effect on the metabolome (Publication III). Additionally, we have characterized two previously unknown thylakoid membrane proteins acetylated by GNAT2 and revealed their surprising role in PSII-LHCII supercomplex dynamics (Publication IV).

5.1 GNAT2 challenges the dogma of protein phosphorylation as the main determinant of state transitions and thylakoid dynamics

As we demonstrate in Publication I, GNAT2 is an active chloroplast-localized acetyltransferase required for state transitions, a process previously thought to be mainly regulated by the reversible phosphorylation of LHCII proteins (Bellaflore et al., 2005; Kyle et al., 1983; Vener et al., 1997). However, the mechanism behind the state transition phenotype of the *gnat2* mutants has remained largely unsolved. Our results clearly show that there is no deficiency in LHCII phosphorylation, but it

rather is markedly increased in *gnat2* (Publications I-III), both for Lhcb1 and Lhcb2. Phosphorylation of a threonine residue (T40) of Lhcb2 together with the two preceding positively charged arginine residues have been shown to be crucial for the interaction between PSI and LHCII (Pan et al., 2018). Interestingly, the Lhcb2.2 isoform was found to be Lys-acetylated on two residues, K42 and K120 in the free LHCII of Col-0 (and *stn7*), while Lys-acetylation was absent in all biological replicates of *gnat2-1* and detected in only one biological replicate of *gnat2-2* (Publication I). Lack of Lys-acetylation would maintain the positive charge of the lysine residue, which in theory could affect the electrostatic environment of the threonine and arginine residues involved in LHCII docking to PSI. However, Lhcb2.2 was not detected among the potential Lys-acetylation targets of GNAT2 in the quantitative Lys-acetylome analysis of whole leaf samples, which together with the detection of Lhcb2.2 Lys-acetylation in one replicate of *gnat2-2* casts some doubt on this hypothesis. However, it is also feasible that in addition to GNAT2, some other chloroplast GNAT can acetylate Lhcb2.2, thus explaining its detection in *gnat2-2*.

In addition to LHCII phosphorylation, the formation of the PSI-LHCII state transition complex requires an intact docking site for LHCII at the PSI-LHCI complex. The PSI docking site is formed by four subunits, PsaH, PsaI, PsaL and PsaO, and defects in their accumulation have been shown to result in impaired state transitions (Jensen et al., 2004; Lunde et al., 2000). Based on the quantitative proteomic analysis in Publication I, no changes were detected in the accumulation of PsaH and PsaL in the *gnat2* mutants compared to Col-0, while PsaO was not detected. Further, immunoblot analysis confirmed that PsaH accumulation was normal in *gnat2* (Publication I: Figure 5). Three PSI docking site proteins (PsaH, PsaL and PsaO) were detected in the proteomic analysis of the PSI/PSII bands excised from blue native gels in Koskela et al. (2020). There, the accumulation of these proteins was unaffected when *gnat2* mutants were compared to Col-0. Although the PSI docking site seems to be unaffected by the inactivation of GNAT2, the question remains whether the small, yet significant, decrease in Lys-acetylation of PsaH (K138) in then *gnat2* mutants has an effect on LHCII docking (Publication I).

The formation of the PSI-LHCII complex is likely facilitated by the loosening of the grana stacks, which has been suggested to be promoted by LHCII phosphorylation (Pietrzykowska et al., 2014; Wood et al., 2018). Thus, inhibition of state transitions by the tighter stacking of grana in *gnat2* is a tempting hypothesis that was tested in Publication II by depleting the thylakoid samples of Mg^{2+} ions, which results in the destacking of the thylakoid membrane. However, the artificial randomization of the thylakoid membrane restored the formation of the PSI-LHCII complex only marginally, indicating that other factors than impaired thylakoid dynamics inhibit state transitions in *gnat2* (Publication II: Figure 4).

5.1.1 Why are grana more tightly packed in the *gnat2* mutant?

The stacking of grana membranes is a co-operative process made possible by the organization of the photosynthetic complexes in the thylakoid membrane together with the vertical electrostatic and van der Waals interactions of the stroma-exposed regions of the PSII-LHCII supercomplexes and LHCII trimers (Albanese et al., 2017; Daum et al., 2012; Nield et al., 2000; Standfuss et al., 2005). More specifically, the positively charged N-termini of the LHCII trimers interact with the negatively charged flat stromal surfaces of the LHCII trimers on the opposing sides of the stromal gap (Standfuss et al., 2005). In addition, specific interactions have been identified between the N-terminal loops of Lhcb1 or Lhcb2 and PSII core proteins as well as the monomeric Lhcb4 proteins (Albanese et al., 2020). Cations are required both for the formation of the PSII-LHCII supercomplexes as well as to counteract the net negative surface charge of the thylakoid membranes, thus enabling their organization into grana stacks (Barber, 1980; Barber & Chow, 1979; Puthiyaveetil et al., 2017).

Phosphorylation of LHCII proteins introduces a negative charge, which increases the electrostatic repulsion transversally between the complexes on the opposing sides of the stromal gap as well as laterally between the PSII-LHCII supercomplexes (Barber, 1982; Puthiyaveetil et al., 2017). The net result of these changes is the loosening of the grana stacks evidenced by a decrease in grana diameter and the number of membrane layers per grana stack, and an increase in the number of grana stacks (Kyle et al., 1983; Rozak et al., 2002; Wood et al., 2018). This, on the other hand, increases the interaction area between the appressed and non-appressed thylakoid membranes (by increasing the area of grana margins and tops), thus likely facilitating the formation of the PSI-LHCII complex (Kyle et al., 1983; Pietrzykowska et al., 2014; Wood et al., 2018) .

The tight packing of grana stacks and the impaired thylakoid dynamics in *gnat2* together with the extensive phosphorylation of the Lhcb proteins (Publications I-III) seem to contradict the idea of LHCII phosphorylation as the main driver of the light induced changes of thylakoid stacking. The contradiction is less stark in the light of results by Puthiyaveetil et al. (2017), who suggest that the effect of phosphorylation on the stromal gap is, nonetheless, surprisingly small, and that additional forces, such as a decrease in cation screening, are involved in the loosening of grana upon high LHCII phosphorylation. Alternatively, changes in the oligomerization of the CURT proteins responsible for inducing thylakoid curvature could participate in the loosening of grana stacks (Armbruster et al., 2013). In the case of *gnat2*, it does seem feasible, that additional cation screening would be required to maintain (and potentially enhance) the tight grana packing, suggesting that ion fluxes might be affected in the mutant. However, further studies are needed to assess the involvement

of ion fluxes in the grana stacking of the *gnat2* mutants. An especially interesting research topic would be the effect of Lys-acetylation on the function of KEA1/2 K^+ transporters (Kunz et al., 2014), that were identified among the potential acetylation targets of GNAT2 (Publication I). The decrease in Lys-acetylation of Lhcb1.4 (and possibly Lhcb2.2) observed in the *gnat2* mutants (Publication I) maintains the positive charge of the Lys-residues, which in theory could also participate in mitigating the electrostatic repulsion introduced by phosphorylation. In the future, comparison of the *gnat2* mutants to the *psal* mutant, which lacks state transitions and exhibits hyperphosphorylation of the LHCII proteins (Lunde et al., 2000; Rantala et al., 2016), could help dissect the GNAT2-specific effect on thylakoid dynamics.

In addition to the increased phosphorylation of LHCII proteins in *gnat2*, an interesting observation is the presence of phosphorylated Lhcb proteins in all LHCII pools (Publication II: Figure 3). Especially intriguing is the detection of (P-)Lhcb2 in the M-LHCII pool, which in Col-0 has been showed to compose mainly of Lhcb1 and Lhcb3 (Galka et al., 2012). In the light of proteomic analysis of free LHCII bands in Publication I and Koskela et al. (2020) it seems that the overall composition of LHCII in the L-LHCII pool is unchanged in the *gnat2* mutants. Similarly, no changes in the accumulation of Lhcb proteins were detected in the proteomic analysis of leaf protein extracts from *gnat2* and Col-0 (Publication I). However, based on the 2D-BN blots presented in Publication II, the distribution of the Lhcb subunits is clearly affected in the *gnat2* mutant. In addition to the presence of (P-)Lhcb2 in the M-LHCII pool, it seems plausible that there is slightly less Lhcb1 and Lhcb3 in M-LHCII in the *gnat2* mutant compared to Col-0 (Publication II; Figure S1.). It should however be noted, that the 2D-BN immunoblot results are more qualitative in nature and should be verified using a quantitative approach. Nonetheless, the notable presence of (P-)Lhcb2 in M-LHCII is a strong indication of altered Lhcb distribution within the LHCII pools. Whether the potential changes in the stoichiometry and phosphorylation of the LHCII trimers would have an effect on thylakoid dynamics remains an interesting topic for future studies.

5.2 Chloroplast GNATs comprise a robust acetylation machinery

GNAT2 is one of seven chloroplast-localized GNAT acetyltransferases (GNAT1-5, GNAT7 and GNAT10) (Publication I, Bienvenut et al., 2020). In addition, GNAT6 has been shown to associate with the chloroplast and the nuclear envelope (Bienvenut et al., 2020). Interestingly, heterologous expression of recombinant chloroplast GNATs in *E.coli* resulted in the accumulation of both Lys- and N-terminally acetylated proteins that were identified using mass spectrometry (Bienvenut et al., 2020). While chloroplast GNATs exhibited rather distinct substrate

specificity as Lys-acetyltransferases, evidenced by the little overlap between the Lys-acetylation targets and the residues surrounding the Lys-acetylation sites of the GNAT enzymes, the N-terminal acetyltransferase specificity was somewhat relaxed (Bienvenut et al., 2020). These results suggest that the GNAT enzymes could share at least some acetylation targets *in planta*.

The relaxed specificity of the chloroplast GNATs likely explains the shared metabolome features identified in Publication III. Especially interesting is the increased levels of the chloroplast MGDG lipids together with the reduced levels of several oxylipins and the JA biosynthesis intermediate dnOPDA (Table 2). MGDG is the most abundant thylakoid membrane lipid that together with digalactosyl diacylglycerol (DGDG) is essential for both thylakoid biosynthesis and photosynthesis (Block et al., 1983; Kobayashi et al., 2007). MGDG is a non-bilayer-forming lipid that has an important role in stabilizing membrane proteins such as LHCII (Seiwert et al., 2017). As the most abundant membrane lipids, MGDG and DGDG also serve as major precursors for the lipid-derived signalling molecules, oxylipins. In addition to having signalling functions of their own, oxylipins are also the precursors for the phytohormone JA (Wasternack & Feussner, 2018). The biosynthesis of JA starts in the chloroplast by the enzymatic hydroperoxidation of polyunsaturated fatty acids (PUFAs) catalysed by the 13-lipoxygenase (13-LOX) enzymes, that specifically produce C-13-oxygenated PUFAs. The C-13-oxygenated PUFA is then converted to a cyclic (dn)OPDA molecule by the action of two chloroplastic enzymes, 13-allene oxide synthase (AOS) and allene oxide cyclase (AOC). (dn)OPDA is then transferred to the peroxisome for the final steps of JA biosynthesis.

Our metabolomic analysis identified several oxylipins with decreased levels, including the likely intermediates of JA biosynthesis, HpOTre and dnOPDA (Publication III). Since the abundance of MGDG (and a few other membrane lipids) was slightly increased in the studied *gnat* mutants, it seems unlikely that the lack of precursors would be behind the decrease in oxylipin levels. Although relatively little is known about the regulation of JA biosynthesis, it has been suggested that PTMs might be involved (Scholz et al., 2015). Interestingly, the predominant 13-LOX enzyme in the leaf, LOX2, has eight and the first committed enzyme of JA biosynthesis, AOS, up to seven Lys-acetylation sites whose function remains unsolved (Publication I, Hartl et al., 2017). Additionally, JA biosynthesis is known to be regulated by the MGDG:DGDG ratio, which based on the increase in MGDG content, might be affected in the *gnat* mutants. However, the coverage of our metabolomic analysis is not sufficient to properly assess the lipid and oxylipin profiles of the *gnat* mutants, and a more detailed study of the lipid and oxylipin composition would be required.

The scarcity of acetylated metabolites identified in our analysis suggests, that chloroplast GNATs likely affect the metabolome mostly indirectly via the acetylation of protein targets. However, this does not rule out the direct involvement of GNATs in metabolite acetylation, but might also be a reflection of the limited capacity of the used method. For example, the known acetylation targets of GNAT1 and GNAT2, (N-acetyl)serine and 5-MT that is acetylated to produce melatonin, were not detected in our analysis (Lee et al., 2014, 2019). The two acetylated metabolites identified in our study, Nα-acetyl-l-arginine in *gnat2* and N-acetylproline in *gnat7,* do raise the intriguing question of the respective GNAT's potential function as amino acid acetyltransferases. In the future, *in vitro* studies of enzyme activity should help to assess the validity of this hypothesis. The physiological role of free acetylated amino acids in the cell also remains a subject for studies to come.

The shared metabolome features and the lack of major changes in the photosynthetic properties in most of the studied *gnat* inactivation lines suggest that the physiological roles of the chloroplast GNATs are likely at least partially complementary (Publication III). This hypothesis is further supported by the relaxed substrate specificity of the chloroplast GNATs as well as by the increased Lys-acetylation of some chloroplast proteins in the *gnat2* mutants (Publication I, Bienvenut et al., 2020). The likely redundancy together with the broad range of acetylation reactions catalysed by the chloroplast GNATs as well as the high number of the GNAT enzymes result in a robust acetylation machinery in the subcellular compartment, highlighting the importance of this PTM in the chloroplast. However, this also means that higher order mutants are likely required to elucidate the physiological function(s) of protein (and possibly metabolite) acetylation in the chloroplast.

5.3 ALM proteins affect the dynamics of the PSII-LHCII supercomplexes

The main components of the photosynthetic electron transfer chain have remained largely unchanged throughout the evolution, but in addition, photosynthetic organisms have evolved a myriad of regulatory mechanisms helping them to adapt to their specific environment. As a consequence, researchers have obtained a relatively detailed understanding of the components of the electron transfer chain, while the regulatory aspects hold many unanswered questions. Due to their high conservation in the green lineage, the two Lys-acetylation targets of GNAT2, ALM-A and ALM-B, appear as interesting candidates potentially involved in photosynthesis regulation (Publication IV).

The co-migration of ALM proteins together with the disconnected M-LHCII complex revealed by the 2D-BN-SDS-PAGE analysis in Publication IV suggests that ALMs might have a role in the function and/or regulation of the LHCII antenna. This hypothesis was supported by structural modelling of M-LHCII together with ALM-A that revealed a potential binding site for ALM between the Lhcb1/Lhcb3 trimer and the Lhcb4 monomer. It must be noted that structural modelling of membrane protein interaction is relatively challenging and the result is simply a prediction that needs to be verified using alternative biochemical methods. Furthermore, additional experiments are required to confirm the orientation of ALM in the thylakoid membrane. Nonetheless, another finding offering some indirect support for the potential interaction of ALM with the M-LHCII complex is the high co-occurrence of *ALM* with *LHCB4* genes observed in our BLASTp analysis of non-flowering plants (Publication IV: Table 1). The monomeric Lhcb4 mediates the interaction of M-LHCII with the PSII core and is found in flowering plants, but has been lost in many non-flowering plant species (Caffarri et al., 2009; Grebe et al., 2019).

Surprisingly, the inactivation of the *ALM* genes results in more intact PSII-LHCII supercomplexes in growth light, and the effect is even more evident after a 4 h high light treatment when the *alm-a/b* mutant is compared to Col-0 (Publication IV: Figure 5). Clear native gel electrophoresis revealed that especially the amount of the C2S2M2 and C2S2M complexes is higher in *alm-a/b* than in Col-0, suggesting that more M-LHCII remains attached to the PSII supercomplexes in the mutant. Despite this, no decrease in the disconnected M-LHCII is observed in *alm-a/b* in the clear native gel. It is possible that the M-LHCII that detaches from the PSII-LHCII supercomplexes is further disassembled into an LHCII trimer and monomerized Lhcb4 and Lhcb6 proteins. Betterle et al. (2009) have suggested that the monomeric Lhcb proteins indeed detach from the M-LHCII trimer under high light. A tempting hypothesis would be that the binding of ALM to M-LHCII could facilitate its detachment from the PSII core, thus enabling the dynamic readjustment of PSII antenna size in response to the prevailing light conditions. Further work is, however, required to assess the validity of this claim. Since ALMs were first identified as Lys-acetylation targets of GNAT2 (Publication I), we were also interested to see whether they might be required for the formation of the state transition complex. However, no changes in the amount of the state transition complex were observed in native gel analysis of *alm-a/b* thylakoid samples (Publication IV: Figure 5), suggesting that ALMs are not involved in the balancing of excitation energy distribution via state transitions.

The potential association of ALM with M-LHCII might further implicate it in the process of NPQ. The disassembly of the M-LHCII complex into its monomeric components has been shown to correlate to NPQ, evidenced by the similar light- and ΔpH- dependence of the processes, as well as the requirement for PsbS (Betterle et

al., 2009). Based on their results, Betterle et al. (2009) suggest that M-LHCII disassembly induces the disassociation of M-LHCII from the PSII-LHCII supercomplexes, thus decreasing the PSII antenna size upon high light intensities. In the light of the increased amount of the C2S2M(2) complexes in the *alm-a/b* mutant, it will be intriguing to take a closer look at the NPQ of the mutant.

6 Conclusions

The aim of this work was to elucidate the physiological role(s) of the newly identified group of chloroplast GNAT acetyltransferases, with a special focus on photosynthesis. To achieve this, I characterized a set of single *gnat* knock-out mutants using a broad range of biochemical and biophyical methods. My work has shown that GNAT2 is required for the balancing of the excitation energy between the photosystems via state transitions (Publication I). In addition, the inactivation of GNAT2 abolishes the light-dependent dynamics of the thylakoid membrane and results in increased phosphorylation of the LHCII proteins (Publication II). All of the chloroplast GNATs investigated in this work (GNAT1, GNAT2, GNAT4, GNAT6, GNAT7 and GNAT10) have a marked effect on the metabolome, and affect the accumulation of e.g. oxylipins, lipids and two acetylated amino acids (Publication III). Finally, I have characterized two previously unknown thylakoid membrane proteins, ALM-A and ALM-B, that are Lys-acetylated by GNAT2 and are involved in PSII-LHCII supercomplex dynamics (Publication IV).

While the results presented in this thesis have uncovered new layers in the regulation of photosynthesis, several open questions remain. More work is needed to solve the molecular mechanism behind the state transition phenotype of *gnat2* and unravel what is causing the impaired thylakoid dynamics in the mutant. The shared metabolome features of the single *gnat* mutants suggest that there is at least some redundancy between the chloroplast GNATs. Studies on higher order GNAT mutants will likely help resolve the physiological roles of the distinct chloroplast acetyltransferases. Also, the involvement of ALM in the adjustment of PSII antenna size (and the effect of Lys-acetylation on ALM) is an intriguing line for future studies.

Acknowledgements

My first thank you goes to my supervisor, Prof. Paula Mulo, for the support and guidance (and the occasional gentle push), but above all for trusting me and letting me find my way of doing science. You have been the best supervisor I could have hoped for. Prof. Eevi Rintamäki is thanked for her guidance throughout my studies and for always being so patient and thorough. I wish to thank my advisory committee members Docent Esa Tyystjärvi and Dr. Michael Wrzaczek for their valuable feedback during my PhD studies. Prof. Laura Jaakola and Docent Alexey Shapiguzov are warmly thanked for critically reviewing my thesis and Assistant Prof. Emilie Wientjes for kindly agreeing to be my opponent.

I am deeply grateful to all the people who have taught, helped and supported me since my first summer at the Molecular Plant Biology unit ten years ago. Sari, Marjaana S. and Vipu are thanked for introducing me to lab work and photosynthesis research. A heartfelt thank you also goes to Vilja for a fun summer with *Actinomyces* (that nonetheless showed me that plants were my thing). Thank you to all the current and past group members: Minna, Magda, Laura, Maisa and Tiia, you have been a pleasure to work with! I am also grateful to Mark Bailey, who is the kindest and most dedicated collaborator I was lucky to meet. Little of this work could have been possible without the technical support from Mika, Eve, Anniina and Tapio R. Thank you for that.

So many people in our work community have not only contributed to my scientific journey, but have also offered friendship and support, especially when life has presented challenges. Some of you are already thanked above (you know who you are), but I would also like to express my gratitude for the friendship of Sanna, Ninni, Moona, Tapio L., Sema and Steffen.

In addition to an extraordinary work community, I am also lucky to have the love and support of all of my friends, especially Martta, Lotta L., Katri, Aliisa and Lotta P., who is also the amazing artist behind the cover of this book. I wouldn't be here without the love from my family, mama, sese and Pentti, who in addition to never doubting me, with their example didn't leave me any other option than pursuing a career in research. I am beyond grateful to Alma and her unborn little brother, who have both turned my world upside down, while at the same time making me more

centered and grounded than I've ever been. And finally, Marjaana, my love, you are a source of inspiration both in work and life and I couldn't be more grateful to get to spend my life with you.

Ajste Date 13.6.2023

List of References

Adams, W. W., Muller, O., Cohu, C. M., & Demmig-Adams, B. (2013). May photoinhibition be a consequence, rather than a cause, of limited plant productivity? *Photosynthesis Research*, *117*(1–3), 31–44.

Albanese, P., Melero, R., Engel, B. D., Grinzato, A., Berto, P., Manfredi, M., Chiodoni, A., Vargas, J., Sorzano, C. Ó. S., Marengo, E., Saracco, G., Zanotti, G., Carazo, J. M., & Pagliano, C. (2017). Pea PSII-LHCII supercomplexes form pairs by making connections across the stromal gap. *Scientific Reports, 7*(1), 1–16.

Albanese, P., Tamara, S., Saracco, G., Scheltema, R. A., & Pagliano, C. (2020). How paired PSII-LHCII supercomplexes mediate the stacking of plant thylakoid membranes unveiled by structural mass-spectrometry. *Nature Communications*, *11*(1).

Altschul, S. F., Gish, W., Miller, W., Myers, E. W., & Lipman, D. J. (1990). Basic local alignment search tool. *Journal of Molecular Biology*, *215*(3), 403–410.

Amunts, A., Drory, O., & Nelson, N. (2007). The structure of a plant photosystem I supercomplex at 3.4 Å resolution. *Nature, 447*, 58–63.

Ancín, M., Millan, A. F. S., Larraya, L., Morales, F., Veramendi, J., Aranjuelo, I., & Farran, I. (2019). Overexpression of thioredoxin m in tobacco chloroplasts inhibits the protein kinase STN7 and alters photosynthetic performance. *Journal of Experimental Botany*, *70*(3), 731–733.

Anderson, J. M. (1982). Distribution of the cytochromes of spinach chloroplasts between the appressed membranes of grana stacks and stroma-exposed thylakoid regions. *FEBS Letters*, *138*(1), 62–66.

Andersson, B., & Anderson, J. M. (1980). Lateral heterogeneity in the distribution of chlorophyll-protein complexes of the thylakoid membranes of spinach chloroplasts. *Biochimica et Biophysica Acta*, *593*(2), 427–440.

Andersson, I., & Backlund, A. (2008). Structure and function of Rubisco. *Plant Physiology and Biochemistry*, *46*(3), 275–291.

Archibald, J. M. (2015). Endosymbiosis and Eukaryotic Cell Evolution. *Current Biology*, *25*(19), 911–921.

Armbruster, U., Labs, M., Pribil, M., Viola, S., Xu, W., Scharfenberg, M., Hertle, A. P., Rojahn, U., Jensen, P. E., Rappaport, F., Joliot, P., Dörmann, P., Wanner, G., & Leister, D. (2013). Arabidopsis CURVATURE THYLAKOID1 proteins modify thylakoid architecture by inducing membrane curvature. *The Plant Cell*, *25*(7), 2661–2678.

Arnao, M. B. & Hernández-Ruiz, J. (2019). Melatonin: a new plant hormone and/or a plant master regulator? *Trends in Plant Science, 24*(1): 38-48.

Aro, E. M., Suorsa, M., Rokka, A., Allahverdiyeva, Y., Paakkarinen, V., Saleem, A., Battchikova, N., & Rintamäki, E. (2005). Dynamics of photosystem II: a proteomic approach to thylakoid protein complexes. *Journal of Experimental Botany*, *56*(411), 347–356.

Aro, E. M., Virgin, I., & Andersson, B. (1993). Photoinhibition of Photosystem II. Inactivation, protein damage and turnover. *Biochimica et Biophysica Acta*, *1143*(2), 113–134.

Baena-González, E., Barbato, R., & Aro, E.-M. (1999). Role of phosphorylation in the repair cycle and oligomeric structure of photosystem II. *Planta, 208*(2), 196-204.

Barber, J. (1980). Membrane surface charges and potentials in relation to photosynthesis. *Biochimica et Biophysica Acta*, *594*(4), 253–308.

Barber, J. (1982). Influence of Surface Charges on thylakoid structure and function. *Annual Review of Plant Physiology*, *33*(1), 261–295.

Barber, J., & Chow, W. S. (1979). A mechanism for controlling the stacking and unstacking of chloroplast thylakoid membranes. *FEBS Letters*, *105*(1), 5–10.

Bassham, J. A. (1971). Photosynthetic carbon metabolism. *Proceedings of the National Academy of Sciences of the United States of America, 68*(11), 2877–2882.

Bellaflore, S., Barneche, F., Peltler, G., & Rochalx, J. D. (2005). State transitions and light adaptation require chloroplast thylakoid protein kinase STN7. *Nature*, *433*, 892–895.

Betterle, N., Ballottari, M., Zorzan, S., de Bianchi, S., Cazzaniga, S., Dall'Osto, L., Morosinotto, T., & Bassi, R. (2009). Light-induced dissociation of an antenna hetero-oligomer is needed for non-photochemical quenching induction. *Journal of Biological Chemistry*, *284*(22), 15255–15266.

Bienvenut, W. V, Brünje, A., Boyer, J., Mühlenbeck, J. S., Bernal, G., Lassowskat, I., Dian, C., Linster, E., Dinh, T. V, Koskela, M. M., Jung, V., Seidel, J., Schyrba, L. K., Ivanauskaite, A., Eirich, J., Hell, R., Schwarzer, D., Mulo, P., Wirtz, M., Meinnel, T., Giglione, C., & Finkemeier, I. (2020). Dual lysine and N-terminal acetyltransferases reveal the complexity underpinning protein acetylation. *Molecular Systems Biology*, *16*(7), 1–23.

Bienvenut, W. V., Sumpton, D., Martinez, A., Lilla, S., Espagne, C., Meinnel, T., & Giglione, C. (2012). Comparative large scale characterization of plant versus mammal proteins reveals similar and idiosyncratic N-α-acetylation features. *Molecular and Cellular Proteomics*, *11*(6), 1–14.

Block, M. A., Dorne, A. J., Joyard, J., & Douce, R. (1983). Preparation and characterization of membrane fractions enriched in outer and inner envelope membranes from spinach chloroplasts. II. Biochemical characterization. *Journal of Biological Chemistry*, *258*(21), 13281–13286.

Bonardi, V., Pesaresi, P., Becker, T., Schleiff, E., Wagner, R., Pfannschmidt, T., Jahns, P., & Leister, D. (2005). Photosystem II core phosphorylation and photosynthetic acclimation require two different protein kinases. *Nature*, *437*, 1179–1182.

Buchanan, B. B. (1980). Role of light in the regulation of chloroplast enzymes. *Annual Review of Plant Physiology*, *31*(1), 341–374.

Buchanan, B. B. (2016). The path to thioredoxin and redox regulation in chloroplasts. *Annual Review of Plant Physiology*, *67*(1), 1-24.

Buchanan, B. B., Gruissem, W., & Jones, R. L. (Eds.) (2015). Biochemistry and molecular biology of plants (2nd ed.). *Wiley-Blackwell,* 542-566.

Byeon, Y., & Back, K. (2016). Low melatonin production by suppression of either serotonin N-acetyltransferase or N-acetylserotonin methyltransferase in rice causes seedling growth retardation with yield penalty, abiotic stress susceptibility, and enhanced coleoptile growth under anoxic conditions. *Journal of Pineal Research*, *60*(3), 348–359.

Cady, C. W., Crabtree, R. H., & Brudvig, G. W. (2008). Functional models for the oxygen-evolving complex of photosystem II. *Coordination Chemistry Reviews*, *252*(3–4), 444-455.

Caffarri, S., Kouřil, R., Kereïche, S., Boekema, E. J., & Croce, R. (2009). Functional architecture of higher plant photosystem II supercomplexes. *The EMBO Journal*, *28*(19), 3052–3063.

Carol, P., Stevenson, D., Bisanz, C., Breitenbach, J., Sandmann, G., Mache, R., Coupland, G., & Kuntz, M. (1999). Mutations in the Arabidopsis Gene IMMUTANS Cause a Variegated Phenotype by Inactivating a Chloroplast Terminal Oxidase Associated with Phytoene Desaturation. *The Plant Cell*, *11*(1), 57–68.

Cazzaniga, S., Dall'Osto, L., Kong, S. G., Wada, M., & Bassi, R. (2013). Interaction between avoidance of photon absorption, excess energy dissipation and zeaxanthin synthesis against photooxidative stress in Arabidopsis. *The Plant Journal*, *76*(4), 568–579.

Chen, J., Wang, P., Mi, H. L., Chen, G. Y., & Xu, D. Q. (2010). Reversible association of ribulose-1, 5-bisphosphate carboxylase/oxygenase activase with the thylakoid membrane depends upon the ATP level and pH in rice without heat stress. *Journal of Experimental Botany*, *61*(11), 2939–2950.

Crepin, A., & Caffarri, S. (2015). The specific localizations of phosphorylated Lhcb1 and Lhcb2 isoforms reveal the role of Lhcb2 in the formation of the PSI-LHCII supercomplex in Arabidopsis during state transitions. *Biochimica et Biophysica Acta*, *1847*(12), 1539–1548.

Crepin, A., & Caffarri, S. (2018). Functions and evolution of Lhcb isoforms composing LHCII, the major light harvesting complex of Photosystem II of green eukaryotic organisms. *Current Protein & Peptide Science*, *19*, 1–15.

Dall'Osto, L., Caffarri, S., & Bassi, R. (2005). A mechanism of nonphotochemical energy dissipation, independent from psbs, revealed by a conformational change in the antenna protein CP26. *The Plant Cell*, *17*(4), 1217–1232.

Daum, B., Nicastro, D., Austin, J., Richard McIntosh, J., & Kühlbrandt, W. (2012). Arrangement of Photosystem II and ATP Synthase in Chloroplast Membranes of Spinach and Pea. *The Plant Cell*, *22*(4), 1299–1312.

Demmig-Adams, B., & Adams, W. W. (1992). Photoprotection and other responses of plants to high light stress. *Annual Review of Plant Physiology and Plant Molecular Biology*, *43*(1), 599–626.

Dinh, T. V., Bienvenut, W. V., Linster, E., Feldman-Salit, A., Jung, V. A., Meinnel, T., Hell, R., Giglione, C., & Wirtz, M. (2015). Molecular identification and functional characterization of the first Nα-acetyltransferase in plastids by global acetylome profiling. *Proteomics*, *15*(14), 2426–2435.

Drazic, A., Myklebust, L. M., Ree, R., & Arnesen, T. (2016). The world of protein acetylation. *Biochimica et Biophysica Acta*, *1864*(10), 1372–1401.

Edgar, R. C. (2004). MUSCLE: multiple sequence alignment with high accuracy and high throughput. *Nucleic Acids Research*, *32*(5), 1792–1797.

Finkemeier, I., Laxa, M., Miguet, L., Howden, A. J. M., & Sweetlove, L. J. (2011). Proteins of diverse function and subcellular location are lysine acetylated in Arabidopsis. *Plant Physiology*, *155*(4), 1779–1790.

Fischer, W. W., Hemp, J., & Johnson, J. E. (2016). Evolution of Oxygenic Photosynthesis. *Annual Review of Earth and Planetary Sciences*, *44*(1), 647–683.

Fristedt, R., Willig, A., Granath, P., Crèvecoeur, M., Rochaix, J. D., & Vener, A. V. (2009). Phosphorylation of photosystem II controls functional macroscopic folding of photosynthetic membranes in Arabidopsis. *The Plant Cell*, *21*(12), 3950–3964.

Galka, P., Santabarbara, S., Khuong, T. T. H., Degand, H., Morsomme, P., Jennings, R. C., Boekema, E. J., & Caffarri, S. (2012). Functional analyses of the plant photosystem I-light-harvesting complex II supercomplex reveal that light-harvesting complex II loosely bound to photosystem ii is a very efficient antenna for photosystem I in state II. *Plant Cell*, *24*(7), 2963–2978.

Gao, X., Hong, H., Li, W. C., Yang, L., Huang, J., Xiao, Y. L., Chen, X. Y., & Chen, G. Y. (2016). Downregulation of Rubisco Activity by Non-enzymatic Acetylation of RbcL. *Molecular Plant*, *9*(7), 1018–1027.

Geigenberger, P., Thormählen, I., Daloso, D. M., & Fernie, A. R. (2017). The unprecedented versatility of the plant thioredoxin system. *Trends in Plant Science*, *22*(3), 249–262.

Gilmore, A. M., & Yamamoto, H. Y. (1991). Resolution of lutein and zeaxanthin using a non-endcapped, lightly carbon-loaded C18 high-performance liquid chromatographic column. *Journal of Chromatography A*, *543*, 137–145.

Goodstein, D. M., Shu, S., Howson, R., Neupane, R., Hayes, R. D., Fazo, J., Mitros, T., Dirks, W., Hellsten, U., Putnam, N., & Rokhsar, D. S. (2012). Phytozome: a comparative platform for green plant genomics. *Nucleic Acids Research*, *40*(1), 1178–1186.

Grebe, S., Trotta, A., Bajwa, A. A., Suorsa, M., Gollan, P. J., Jansson, S., Tikkanen, M., & Aro, E. M. (2019). The unique photosynthetic apparatus of Pinaceae: analysis of photosynthetic complexes in Picea abies. *Journal of Experimental Botany*, *70*(12), 3211–3225.

Grieco, M., Suorsa, M., Jajoo, A., Tikkanen, M., & Aro, E. M. (2015). Light-harvesting II antenna trimers connect energetically the entire photosynthetic machinery — including both photosystems II and I. *Biochimica et Biophysica Acta*, *1847*(6–7), 607–619.

Hahn, A., Vonck, J., Mills, D. J., Meier, T., & Kühlbrandt, W. (2018). Structure, mechanism, and regulation of the chloroplast ATP synthase. *Science*, *360*(6389), 4318.

Hanke, G., & Mulo, P. (2013). Plant type ferredoxins and ferredoxin-dependent metabolism. *Plant, Cell & Environment*, *36*(6), 1071–1084.

Hartl, M., Füßl, M., Boersema, P. J., Jost, J., Kramer, K., Bakirbas, A., Sindlinger, J., Plöchinger, M., Leister, D., Uhrig, G., Moorhead, G. B., Cox, J., Salvucci, M. E., Schwarzer, D., Mann, M., & Finkemeier, I. (2017). Lysine acetylome profiling uncovers novel histone deacetylase substrate proteins in Arabidopsis. *Molecular Systems Biology*, *13*(10), 949.

Haußühl, K., Andersson, B., & Adamska, I. (2001). A chloroplast DegP2 protease performs the primary cleavage of the photodamaged D1 protein in plant photosystem II. *The EMBO Journal*, *20*(4), 713–722.

Hiller, K., Grote, A., Scheer, M., Münch, R., & Jahn, D. (2004). PrediSi: prediction of signal peptides and their cleavage positions. *Nucleic Acids Research*, *32*(2), 375-379.

Holleboom, C. P., & Walla, P. J. (2014). The back and forth of energy transfer between carotenoids and chlorophylls and its role in the regulation of light harvesting. *Photosynthesis Research*, *119*(1–2), 215–221.

Hoshiyasu, S., Kohzuma, K., Yoshida, K., Fujiwara, M., Fukao, Y., Akiho Yokota, & Akashi, K. (2013). Potential involvement of N-terminal acetylation in the quantitative regulation of the ε subunit of chloroplast ATP synthase under drought stress. *Bioscience, Biotechnology and Biochemistry*, *77*(5), 998–1007.

Hruz, T., Laule, O., Szabo, G., Wessendorp, F., Bleuler, S., Oertle, L., Widmayer, P., Gruissem, W., & Zimmermann, P. (2008). Genevestigator v3: a reference expression database for the meta-analysis of transcriptomes. *Advances in Bioinformatics*, 1–5.

Hwang, O. J., & Back, K. (2020). Simultaneous suppression of two distinct serotonin N-acetyltransferase isogenes by RNA interference leads to severe decreases in melatonin and accelerated seed deterioration in rice. *Biomolecules*, *10*(1), 141.

Ivanov, A. G., Rosso, D., Savitch, L. V., Stachula, P., Rosembert, M., Oquist, G., Hurry, V., & Hüner, N. P. A. (2012). Implications of alternative electron sinks in increased resistance of PSII and PSI photochemistry to high light stress in cold-acclimated *Arabidopsis thaliana*. *Photosynthesis Research*, *113*(1–3), 191–206.

Jansson, S. (1999). A guide to the Lhc genes and their relatives in Arabidopsis. *Trends in Plant Science*, *4*(6), 236–240.

Järvi, S., Suorsa, M., Paakkarinen, V., & Aro, E. M. (2011). Optimized native gel systems for separation of thylakoid protein complexes: novel super- and mega-complexes. *Biochemical Journal*, *439*(2), 207–214.

Jensen, P. E., Haldrup, A., Zhang, S., & Scheller, H. V. (2004). The PSI-O subunit of plant photosystem I is involved in balancing the excitation pressure between the two photosystems. *Journal of Biological Chemistry*, *279*(23), 24212–24217.

Johnson, M. P., & Ruban, A. V. (2011). Restoration of rapidly reversible photoprotective energy dissipation in the absence of PsbS protein by enhanced ΔpH. *Journal of Biological Chemistry*, *286*(22), 19973–19981.

Johnson, M. P., & Wientjes, E. (2020). The relevance of dynamic thylakoid organisation to photosynthetic regulation. *Biochimica et Biophysica Acta*, *1861*(4), 148039.

Kanervo, E., Spetea, C., Nishiyama, Y., Murata, N., Andersson, B., & Aro, E. M. (2003). Dissecting a cyanobacterial proteolytic system: efficiency in inducing degradation of the D1 protein of photosystem II in cyanobacteria and plants. *Biochimica et Biophysica Acta*, *1607*(2–3), 131–140.

Kirchhoff, H., Li, M., & Puthiyaveetil, S. (2017). Sublocalization of cytochrome b_6f complexes in photosynthetic membranes. *Trends in Plant Science*, *22*(7), 574–582.

Kobayashi, K., Kondo, M., Fukuda, H., Nishimura, M., & Ohta, H. (2007). Galactolipid synthesis in chloroplast inner envelope is essential for proper thylakoid biogenesis, photosynthesis, and

embryogenesis. *Proceedings of the National Academy of Sciences of the United States of America*, *104*(43), 17216–17221.

Koskela, M. M., Brünje, A., Ivanauskaite, A., Lopez, L. S., Schneider, D., DeTar, R. A., Kunz, H. H., Finkemeier, I., & Mulo, P. (2020). Comparative analysis of thylakoid protein complexes in state transition mutants nsi and stn7: focus on PSI and LHCII. *Photosynthesis Research*, *145*(1), 15–30.

Kouřil, R., Zygadlo, A., Arteni, A. A., De Wit, C. D., Dekker, J. P., Jensen, P. E., Scheller, H. V., & Boekema, E. J. (2005). Structural characterization of a complex of photosystem I and light-harvesting complex II of *Arabidopsis thaliana*. *Biochemistry*, *44*(33), 10935–10940.

Kowalczyk, N., Rappaport, F., Boyen, C., Wollman, F. A., Collén, J., & Joliot, P. (2013). Photosynthesis in *Chondrus crispus*: The contribution of energy spill-over in the regulation of excitonic flux. *Biochimica et Biophysica Acta*, *1827*(7), 834–842.

Kunz, H. H., Gierth, M., Herdean, A., Satoh-Cruz, M., Kramer, D. M., Spetea, C., & Schroeder, J. I. (2014). Plastidial transporters KEA1, -2, and -3 are essential for chloroplast osmoregulation, integrity, and pH regulation in Arabidopsis. *Proceedings of the National Academy of Sciences of the United States of America*, *111*(20), 7480–7485.

Kurisu, G., Zhang, H., Smith, J. L., & Cramer, W. A. (2003). Structure of the cytochrome b_6f complex of oxygenic photosynthesis: tuning the cavity. *Science*, *302*(5647), 1009–1014.

Kyle, D. J., Staehelin, L. A., & Arntzen, C. J. (1983). Lateral mobility of the light-harvesting complex in chloroplast membranes controls excitation energy distribution in higher plants. *Archives of Biochemistry and Biophysics*, *222*(2), 527–541.

Laemmli, U. K. (1970). Cleavage of structural proteins during the assembly of the head of bacteriophage T4. *Nature, 227*, 680–685.

Lee, H. Y., & Back, K. (2018). Melatonin induction and its role in high light stress tolerance in *Arabidopsis thaliana*. *Journal of Pineal Research*, *65*(3), 1–13.

Lee, H. Y., Byeon, Y., Lee, K., Lee, H. J., & Back, K. (2014). Cloning of Arabidopsis serotonin N-acetyltransferase and its role with caffeic acid O-methyltransferase in the biosynthesis of melatonin in vitro despite their different subcellular localizations. *Journal of Pineal Research*, *57*(4), 418–426.

Lee, H. Y., Byeon, Y., Tan, D. X., Reiter, R. J., & Back, K. (2015). Arabidopsis serotonin N-acetyltransferase knockout mutant plants exhibit decreased melatonin and salicylic acid levels resulting in susceptibility to an avirulent pathogen. *Journal of Pineal Research*, *58*(3), 291–299.

Lee, H. Y., Lee, K., & Back, K. (2019). Knockout of arabidopsis serotonin N-acetyltransferase-2 reduces melatonin levels and delays flowering. *Biomolecules*, *9*(11), 1–12.

Lehtimäki, N., Koskela, M. M., Dahlström, K. M., Pakula, E., Lintala, M., Scholz, M., Hippler, M., Hanke, G. T., Rokka, A., Battchikova, N., Salminen, T. A., & Mulo, P. (2014). Posttranslational modifications of FERREDOXIN-NADP+ OXIDOREDUCTASE in Arabidopsis chloroplasts. *Plant Physiology*, *166*(4), 1764–1776.

Lennon, A. M., Prommeenate, P., & Nixon, P. J. (2003). Location, expression and orientation of the putative chlororespiratory enzymes, Ndh and IMMUTANS, in higher-plant plastids. *Planta*, *218*(2), 254–260.

Lindahl, M., Tabak, S., Cseke, L., Pichersky, E., Andersson, B., & Adam, Z. (1996). Identification, characterization, and molecular cloning of a homologue of the bacterial FtsH protease in chloroplasts of higher plants. *The Journal of Biological Chemistry*, *271*(46), 29329–29334.

Lunde, C., Jensen, P. E., Haldrup, A., Knoetzel, J., & Scheller, H. V. (2000). The PSI-H subunit of photosystem I is essential for state transitions in plant photosynthesis. *Nature, 408*, 613–615.

Lu, Y., Hall, D. A., & Last, R. L. (2011). A small zinc finger thylakoid protein plays a role in maintenance of photosystem II in *Arabidopsis thaliana*. *The Plant Cell*, *23*(5), 1861–1875.

Madeira, F., Pearce, M., Tivey, A. R. N., Basutkar, P., Lee, J., Edbali, O., Madhusoodanan, N., Kolesnikov, A., & Lopez, R. (2022). Search and sequence analysis tools services from EMBL-EBI in 2022. *Nucleic Acids Research*, *50*(1), 276–279.

Malnoë, A., Schultink, A., Shahrasbi, S., Rumeau, D., Havaux, M., & Niyogi, K. K. (2018). The plastid lipocalin LCNP is required for sustained photoprotective energy dissipation in Arabidopsis. *The Plant Cell*, *30*(1), 196–208.

Malone, L. A., Proctor, M. S., Hitchcock, A., Hunter, C. N., & Johnson, M. P. (2021). Cytochrome b_6f – orchestrator of photosynthetic electron transfer. *Biochimica et Biophysica Acta*, *1862*(5), 148380.

Michel, H., Hunt, D. F., Shabanowitz, J., & Bennett, J. (1988). Tandem mass spectrometry reveals that three photosystem II proteins of spinach chloroplasts contain N-acetyl-O-phosphothreonine at their NH2 termini. *The Journal of Biological Chemistry*, *263*(3), 1123–1130.

Mirdita, M., Schütze, K., Moriwaki, Y., Heo, L., Ovchinnikov, S., & Steinegger, M. (2022). ColabFold: making protein folding accessible to all. *Nature Methods*, *19*(6), 679–682.

Munekage, Y., Hashimoto, M., Miyake, C., Tomizawa, K. I., Endo, T., Tasaka, M., & Shikanai, T. (2004). Cyclic electron flow around photosystem I is essential for photosynthesis. *Nature*, *429*, 579–582.

Munekage, Y., Hojo, M., Meurer, J., Endo, T., Tasaka, M., & Shikanai, T. (2002). PGR5 is involved in cyclic electron flow around photosystem I and is essential for photoprotection in Arabidopsis. *Cell*, *110*(3), 361–371.

Murakami, S., & Packer, L. (1971). The role of cations in the organization of chloroplast membranes. *Archives of Biochemistry and Biophysics*, *146*(1), 337–347.

Mustárdy, L., & Garab, G. (2003). Granum revisited. A three-dimensional model – where things fall into place. *Trends in Plant Science*, *8*(3), 117–122.

Nield, J., Orlova, E. V., Morris, E. P., Gowen, B., Van Heel, M., & Barber, J. (2000). 3D map of the plant photosystem II supercomplex obtained by cryoelectron microscopy and single particle analysis. *Nature Structural Biology, 7*(1), 44–47.

Nikkanen, L., & Rintamäki, E. (2019). Chloroplast thioredoxin systems dynamically regulate photosynthesis in plants. *Biochemical Journal*, *476*(7), 1159–1172.

Nikkanen, L., Toivola, J., Trotta, A., Diaz, M. G., Tikkanen, M., Aro, E. M., & Rintamäki, E. (2018). Regulation of cyclic electron flow by chloroplast NADPH-dependent thioredoxin system. *Plant Direct*, *2*(11), e00093.

Nilkens, M., Kress, E., Lambrev, P., Miloslavina, Y., Müller, M., Holzwarth, A. R., & Jahns, P. (2010). Identification of a slowly inducible zeaxanthin-dependent component of non-photochemical quenching of chlorophyll fluorescence generated under steady-state conditions in Arabidopsis. *Biochimica et Biophysica Acta*, *1797*(4), 466–475.

O'Leary, B. M., Scafaro, A. P., Fenske, R., Duncan, O., Ströher, E., Petereit, J., & Millar, A. H. (2020). Rubisco lysine acetylation occurs at very low stoichiometry in mature Arabidopsis leaves: implications for regulation of enzyme function. *The Biochemical Journal*, *477*(19), 3885–3896.

Pan, X., Ma, J., Su, X., Cao, P., Chang, W., Liu, Z., Zhang, X., & Li, M. (2018). Structure of the maize photosystem I supercomplex with light-harvesting complexes I and II. *Science*, *360*(6393), 1109–1113.

Paolillo, D. J. (1970). The three-dimensional arrangement of intergranal lamellae in chloroplasts. *Journal of Cell Science*, *6*(1), 243–253.

Pesaresi, P., Hertle, A., Pribil, M., Kleine, T., Wagner, R., Strissel, H., Ihnatowicz, A., Bonardi, V., Scharfenberg, M., Schneider, A., Pfannschmidt, T., & Leister, D. (2009). Arabidopsis STN7 kinase provides a link between short- and long-term photosynthetic acclimation. *The Plant Cell*, *21*(8), 2402–2423.

Pietrzykowska, M., Suorsa, M., Semchonok, D. A., Tikkanen, M., Boekema, E. J., Aro, E. M., & Jansson, S. (2014). The light-harvesting chlorophyll a/b binding proteins Lhcb1 and Lhcb2 play complementary roles during state transitions in Arabidopsis. *The Plant Cell*, *26*(9), 3646.

Porra, R. J., Thompson, W. A., & Kriedemann, P. E. (1989). Determination of accurate extinction coefficients and simultaneous equations for assaying chlorophylls a and b extracted with four different solvents: verification of the concentration of chlorophyll standards by atomic absorption spectroscopy. *Biochimica et Biophysica Acta*, *975*(3), 384–394.

Portis, A. R. (2003). Rubisco activase - Rubisco's catalytic chaperone. *Photosynthesis Research*, *75*(1), 11–27.

Pribil, M., Pesaresi, P., Hertle, A., Barbato, R., & Leister, D. (2010). Role of plastid protein phosphatase TAP38 in LHCII dephosphorylation and thylakoid electron flow. *PLOS Biology*, *8*(1), e1000288.

Puthiyaveetil, S., Van Oort, B., & Kirchhoff, H. (2017). Surface charge dynamics in photosynthetic membranes and the structural consequences. *Nature Plants, 3*(4), 1–9.

Rantala, M., Lehtimäki, N., Aro, E. M., & Suorsa, M. (2016). Downregulation of TAP38/PPH1 enables LHCII hyperphosphorylation in Arabidopsis mutant lacking LHCII docking site in PSI. *FEBS Letters*, *590*(6), 787–794.

Rantala, M., Tikkanen, M., & Aro, E. M. (2017). Proteomic characterization of hierarchical megacomplex formation in Arabidopsis thylakoid membrane. *The Plant Journal*, *92*(5), 951–962.

Rathore, O. S., Faustino, A., Prudêncio, P., Van Damme, P., Cox, C. J., & Martinho, R. G. (2016). Absence of N-terminal acetyltransferase diversification during evolution of eukaryotic organisms. *Scientific Reports, 6*(1), 1–13.

Rintamäki, E., Kettunen, R., & Aro, E. M. (1996). Differential D1 dephosphorylation in functional and photodamaged photosystem II centers. Dephosphorylation is a prerequisite for degradation of damaged D1. *The Journal of Biological Chemistry*, *271*(25), 14870–14875.

Rintamäki, E., Martinsuo, P., Pursiheimo, S., & Aro, E. M. (2000). Cooperative regulation of light-harvesting complex II phosphorylation via the plastoquinol and ferredoxin-thioredoxin system in chloroplasts. *Proceedings of the National Academy of Sciences of the United States of America*, *97*(21), 11644–11649.

Rokka, A., Suorsa, M., Saleem, A., Battchikova, N., & Aro, E. M. (2005). Synthesis and assembly of thylakoid protein complexes: multiple assembly steps of photosystem II. *The Biochemical Journal*, *388*(1), 159–166.

Rozak, P. R., Seiser, R. M., Wacholtz, W. F., & Wise, R. R. (2002). Rapid, reversible alterations in spinach thylakoid appression upon changes in light intensity. *Plant, Cell & Environment*, *25*(3), 421–429.

Ruban, A. V., & Johnson, M. P. (2009). Dynamics of higher plant photosystem cross-section associated with state transitions. *Photosynthesis Research*, *99*(3), 173–183.

Ruban, A. V., & Johnson, M. P. (2015). Visualizing the dynamic structure of the plant photosynthetic membrane. *Nature Plants, 1*(11), 1–9.

Samol, I., Shapiguzov, A., Ingelsson, B., Fucile, G., Crèvecoeur, M., Vener, A. V., Rochaix, J. D., & Goldschmidt-Clermont, M. (2012). Identification of a photosystem II phosphatase involved in light acclimation in Arabidopsis. *The Plant Cell*, *24*(6), 2596–2609.

Scholz, S. S., Reichelt, M., Boland, W., & Mithöfer, A. (2015). Additional evidence against jasmonate-induced jasmonate induction hypothesis. *Plant Science*, *239*, 9–14.

Schreiber, U., & Klughammer, C. (2008). New accessory for the Dual-PAM-100: The P515 / 535 module and examples of its application. *PAM Application Notes*, *10*, 1–10.

Seiwert, D., Witt, H., Janshoff, A., & Paulsen, H. (2017). The non-bilayer lipid MGDG stabilizes the major light-harvesting complex (LHCII) against unfolding. *Scientific Reports, 7*(1), 1–10.

Shapiguzov, A., Ingelsson, B., Samol, I., Andres, C., Kessler, F., Rochaix, J. D., Vener, A. V., & Goldschmidt-Clermont, M. (2010). The PPH1 phosphatase is specifically involved in LHCII dephosphorylation and state transitions in Arabidopsis. *Proceedings of the National Academy of Sciences of the United States of America*, *107*(10), 4782–4787.

Shikanai, T., Endo, T., Hashimoto, T., Yamada, Y., Asada, K., & Yokota, A. (1998). Directed disruption of the tobacco ndhB gene impairs cyclic electron flow around photosystem I. *Proceedings of the National Academy of Sciences of the United States of America*, *95*(16), 9705–9709.

Standfuss, J., Van Scheltinga, A. C. T., Lamborghini, M., & Kühlbrandt, W. (2005). Mechanisms of photoprotection and nonphotochemical quenching in pea light-harvesting complex at 2.5 A resolution. *The EMBO Journal*, *24*(5), 919–928.

Stepien, P., & Johnson, G. N. (2018). Plastid terminal oxidase requires translocation to the grana stacks to act as a sink for electron transport. *Proceedings of the National Academy of Sciences of the United States of America*, *115*(38), 9634–9639.

Suorsa, M., Järvi, S., Grieco, M., Nurmi, M., Pietrzykowska, M., Rantala, M., Kangasjärvi, S., Paakkarinen, V., Tikkanen, M., Jansson, S., & Aro, E. M. (2012). PROTON GRADIENT REGULATION5 is essential for proper acclimation of Arabidopsis photosystem I to naturally and artificially fluctuating light conditions. *The Plant Cell*, *24*(7), 2934–2948.

Suorsa, M., Rantala, M., Danielsson, R., Järvi, S., Paakkarinen, V., Schröder, W. P., Styring, S., Mamedov, F., & Aro, E. M. (2014). Dark-adapted spinach thylakoid protein heterogeneity offers insights into the photosystem II repair cycle. *Biochimica et Biophysica Acta*, *1837*(9), 1463–1471.

Su, X., Ma, J., Wei, X., Cao, P., Zhu, D., Chang, W., Liu, Z., Zhang, X., & Li, M. (2017). Structure and assembly mechanism of plant C2S2M2-type PSII-LHCII supercomplex. *Science*, *357*(6353), 815–820.

Sylak-Glassman, E. J., Malnoe, A., De Re, E., Brooks, M. D., Fischer, A. L., Krishna, K., & Fleming, G. R. (2014). Distinct roles of the photosystem II protein PsbS and zeaxanthin in the regulation of light harvesting in plants revealed by fluorescence lifetime snapshots. *Proceedings of the National Academy of Sciences of the United States of America*, *111*(49), 17498–17503.

Thormählen, I., Meitzel, T., Groysman, J., Öchsner, A. B., Von Roepenack-Lahaye, E., Naranjo, B., Cejudo, F. J., & Geigenberger, P. (2015). Thioredoxin f1 and NADPH-dependent thioredoxin reductase C have overlapping functions in regulating photosynthetic metabolism and plant growth in response to varying light conditions. *Plant Physiology*, *169*(3), 1766–1786.

Tikkanen, M., Grieco, M., Kangasjärvi, S., & Aro, E. M. (2010). Thylakoid protein phosphorylation in higher plant chloroplasts optimizes electron transfer under fluctuating light. *Plant Physiology*, *152*(2), 723–735.

Tikkanen, M., Mekala, N. R., & Aro, E. M. (2014). Photosystem II photoinhibition-repair cycle protects Photosystem I from irreversible damage. *Biochimica et Biophysica Acta*, *1837*(1), 210–215.

Tikkanen, M., Nurmi, M., Kangasjärvi, S., & Aro, E. M. (2008). Core protein phosphorylation facilitates the repair of photodamaged photosystem II at high light. *Biochimica et Biophysica Acta*, *1777*(11), 1432–1437.

Tikkanen, M., Piippo, M., Suorsa, M., Sirpio, S., Mulo, P., Vainonen, J., Vener, A., Allahverdiyeva, Y., & Aro, E.-M. (2006). State transitions revisited - a buffering system for dynamic low light acclimation of Arabidopsis. *Plant Molecular Biology*, *62*(4–5), 779–793.

Tiwari, A., Mamedov, F., Grieco, M., Suorsa, M., Jajoo, A., Styring, S., Tikkanen, M., & Aro, E. M. (2016). Photodamage of iron–sulphur clusters in photosystem I induces non-photochemical energy dissipation. *Nature Plants, 2*(4), 1–9.

Tóth, T. N., Rai, N., Solymosi, K., Zsiros, O., Schröder, W. P., Garab, G., Van Amerongen, H., Horton, P., & Kovács, L. (2016). Fingerprinting the macro-organisation of pigment–protein complexes in plant thylakoid membranes in vivo by circular-dichroism spectroscopy. *Biochimica et Biophysica Acta*, *1857*(9), 1479–1489.

Tsirigos, K. D., Peters, C., Shu, N., Käll, L., & Elofsson, A. (2015). The TOPCONS web server for consensus prediction of membrane protein topology and signal peptides. *Nucleic Acids Research*, *43*(1), 401–407.

Tyystjärvi, E., & Aro, E. M. (1996). The rate constant of photoinhibition, measured in lincomycin-treated leaves, is directly proportional to light intensity. *Proceedings of the National Academy of Sciences of the United States of America*, *93*(5), 2213–2218.

Ud-Din, A. I. M. S., Tikhomirova, A., & Roujeinikova, A. (2016). Structure and functional diversity of GCN5-related N-acetyltransferases (GNAT). *International Journal of Molecular Sciences, 17*(7), 1018.

Vainonen, J. P., Hansson, M., & Vener, A. V. (2005). STN8 protein kinase in *Arabidopsis thaliana* is specific in phosphorylation of photosystem II core proteins. *The Journal of Biological Chemistry*, *280*(39), 33679–33686

Van Bezouwen, L. S., Caffarri, S., Kale, R., Kouřil, R., Thunnissen, A. M. W. H., Oostergetel, G. T., & Boekema, E. J. (2017). Subunit and chlorophyll organization of the plant photosystem II supercomplex. *Nature Plants, 3*(7), 1–11.

Vener, A. V., Van Kan, P. J. M., Rich, P. R., Ohad, I., & Andersson, B. (1997). Plastoquinol at the quinol oxidation site of reduced cytochrome bf mediates signal transduction between light and protein phosphorylation: thylakoid protein kinase deactivation by a single-turnover flash. *Proceedings of the National Academy of Sciences of the United States of America*, *94*(4), 1585–1590.

Wasternack, C., & Feussner, I. (2018). The Oxylipin Pathways: Biochemistry and Function. *Annual Review of Plant Biology*, *69*, 363–386.

Waterhouse, A. M., Procter, J. B., Martin, D. M. A., Clamp, M., & Barton, G. J. (2009). Jalview Version 2 — a multiple sequence alignment editor and analysis workbench. *Bioinformatics*, *25*(9), 1189–1191.

Wei, J., Li, D. X, Zhang, J. R., Shan, C., Rengel, Z., Song, Z. B. & Chen Q. (2018). Phytomelatonin receptor PMTR1-mediated signaling regulates stomatal closure in *Arabidopsis thaliana*. *Journal of Pineal Research, 65*(2):e12500.

Wientjes, E., Van Amerongen, H., & Croce, R. (2013). LHCII is an antenna of both photosystems after long-term acclimation. *Biochimica et Biophysica Acta*, *1827*(3), 420–426.

Wood, W. H. J., Barnett, S. F. H., Flannery, S., Hunter, C. N., & Johnson, M. P. (2019). Dynamic thylakoid stacking is regulated by LHCII phosphorylation but not its interaction with PSI. *Plant Physiology*, *180*(4), 2152–2166.

Wood, W. H. J., MacGregor-Chatwin, C., Barnett, S. F. H., Mayneord, G. E., Huang, X., Hobbs, J. K., Hunter, C. N., & Johnson, M. P. (2018). Dynamic thylakoid stacking regulates the balance between linear and cyclic photosynthetic electron transfer. *Nature Plants, 4*(2), 116–127.

Wu, X., Oh, M. H., Schwarz, E. M., Larue, C. T., Sivaguru, M., Imai, B. S., Yau, P. M., Ort, D. R., & Huber, S. C. (2011). Lysine acetylation is a widespread protein modification for diverse proteins in Arabidopsis. *Plant Physiology*, *155*(4), 1769–1778.

Xiong, Y., Peng, X., Cheng, Z., Liu, W., & Wang, G. L. (2016). A comprehensive catalog of the lysine-acetylation targets in rice (*Oryza sativa*) based on proteomic analyses. *Journal of Proteomics*, *138*, 20–29.

Xue, C., Liu, S., Chen, C., Zhu, J., Yang, X., Zhou, Y., Guo, R., Liu, X., & Gong, Z. (2018). Global proteome analysis links lysine acetylation to diverse functions in *Oryza Sativa*. *Proteomics*, *18*(1).

Yamamoto, T., Burke, J., Autz, G., & Jagendorf, A. T. (1981). Bound Ribosomes of pea chloroplast thylakoid membranes: location and release *in vitro* by high salt, puromycin, and RNase. *Plant Physiology*, *67*(5), 940–949.

Zhang, L., Paakkarinen, V., Van Wijk, K. J., & Aro, E. M. (1999). Co-translational assembly of the D1 protein into photosystem II. *The Journal of Biological Chemistry*, *274*(23), 16062–16067.

Zhang, Y., Song, L., Liang, W., Mu, P., Wang, S., & Lin, Q. (2016). Comprehensive profiling of lysine acetylproteome analysis reveals diverse functions of lysine acetylation in common wheat. *Scientific Reports*, *6,* 21069.

Zybailov, B., Rutschow, H., Friso, G., Rudella, A., Emanuelsson, O., Sun, Q., & van Wijk, K. J. (2008). Sorting signals, N-terminal modifications and abundance of the chloroplast proteome. *PloS One*, *3*(4).

TURUN
YLIOPISTO
UNIVERSITY
OF TURKU

Painosalama Oy, Turku, Finland 2023

ISBN 978-951-29-9357-4 (PRINT)
ISBN 978-951-29-9358-1 (PDF)
ISSN 0082-7002 (Print)
ISSN 2343-3175 (Online)